Scientific Publishing House

Trends in Ecological and Indoor Environmental Engineering

Njoku Anthony Chinemerem et al. *TEIEE 4(3) 2026*

RESEARCH ARTICLE **OPEN ACCESS**
https://doi.org/10.62622/TEIEE.026.4.3.35-54 **ISSN 2956-9761**

PETROLEUM-DRIVEN HYDROGEOCHEMICAL ALTERATION AND GROUNDWATER CONTAMINATION IN AN OFFSHORE NIGER DELTA DEPOBELT: AN INTEGRATED MULTIVARIATE STATISTICAL, WATER QUALITY INDEX, AND GEOSPATIAL ENGINEERING ASSESSMENT

Njoku Anthony Chinemerem[1], Izeze Elijah Ovie[1*], Chinedu Christian Iheanacho[2], Micheal Abimbola Oladosu[3*], Moses Adondua Abah[4], Chigozirim Steve Amadi[5], Joseph Ezeani[6], Ezekiel Izudike Odimgbe[7]

[1]Department of Geology, Federal University of Petroleum Resources Effurun, Delta State, Nigeria
[2]Department of Microbiology, Faculty of Biosciences, Federal University Wukari, Wukari, Taraba State, Nigeria
[3]Department of Chemical Sciences, Faculty of Science, Anchor University Lagos, Lagos, Nigeria
[4]Department of Biochemistry, Faculty of Pure and Applied Sciences, Federal University Wukari, Wukari, Taraba State, Nigeria
[5]Department of Biochemistry, Faculty of Science, Rivers State University, Port Harcourt, Rivers State, Nigeria
[6]Department of Chemical Engineering, Faculty of Engineering, University of Toledo, Toledo, United States
[7]Department of Healthcare Administration and Risk Management, Faculty of Health Sciences, Ohio Dominican University, Columbus, OH, United States
*Corresponding email: izeze.ovie@fupre.edu.ng; mikeoladosu@gmail.com; moladosu@aul.edu.ng

Received: 15.06.2026; ***Accepted:*** 11.07.2026; ***Available online:*** 31.08.2026; ***Published:*** 30.09.2026

Cite this article: Chinemerem, N. A., Ovie, I. E., Iheanacho, C. C., Oladosu, M. A. Abah, M. A., Amadi, C. S., Ezeani, J., & Odimgbe, E. I. (2026). Petroleum-Driven Hydrogeochemical Alteration and Groundwater Contamination in an Offshore Niger Delta Depobelt: An Integrated Multivariate Statistical, Water Quality Index, and Geospatial Engineering Assessment. *Trends in Ecological and Indoor Environmental Engineering*, 4(3), 35–54.

Background: Groundwater is the principal source of freshwater for many communities in the Niger Delta, where intensive petroleum exploration and production have raised increasing concerns regarding groundwater contamination. Although numerous hydrogeochemical investigations have been conducted within the region, most have focused on onshore environments, leaving offshore groundwater systems largely unexplored. Moreover, the combined application of complementary hydrogeochemical, statistical, index-based, and spatial analytical approaches remains limited, restricting comprehensive evaluation of groundwater quality and contamination patterns. **Objectives:** This study aimed to comprehensively assess groundwater quality and hydrogeochemical characteristics in an offshore petroleum-producing field of the Niger Delta and to identify the dominant natural hydrogeochemical processes and petroleum-related anthropogenic influences governing groundwater chemistry and contamination patterns. **Methods:** Groundwater samples were collected from ten monitoring wells during the dry season of 2024. Physicochemical properties, major ions, heavy metals, and total hydrocarbon content were determined following APHA standard methods with comprehensive QA/QC procedures. Hydrogeochemical facies were evaluated using Piper, Durov, and Stiff diagrams. Pearson correlation, Principal Component Analysis (PCA), and Hierarchical Cluster Analysis (HCA) were applied to identify relationships among hydrochemical variables and classify groundwater samples. Groundwater quality was assessed using the Metal Index (MI) and Water Quality Index (WQI), while Geographic Information System (GIS)-based inverse distance weighting (IDW) interpolation was employed to evaluate the spatial distribution of key groundwater quality indicators. **Results:** Groundwater was consistently characterized by a magnesium-sulphate (Mg–SO_4) hydrochemical facies across all sampling locations. Electrical conductivity (852–1,842 µS/cm), total dissolved solids (1,082–2,338 mg/L), magnesium (98–210 mg/L), sulphate (210–620 mg/L), and iron (2.84–12.45 mg/L) exceeded recommended guideline values in most samples. Principal Component Analysis extracted three components explaining 83.1% of the total variance, representing groundwater mineralisation, salinity-related processes, and sulphate-phosphate enrichment. Hierarchical Cluster Analysis classified the ten wells into four hydro-chemically distinct groups with contamination severity increasing near petroleum infrastructure. Metal Index values ranged from 0.94 to 4.82 (Classes II–V), while Water Quality Index values ranged from 105 to 284, classifying all groundwater samples as unsuitable for drinking without treatment. Geospatial analysis identified contamination hotspots within approximately 500 m of petroleum facilities. **Conclusion:** The findings suggest that groundwater quality in Offshore Field X is governed by the combined influence of natural hydrogeochemical processes and petroleum-related activities. The integrated framework, incorporating hydrogeochemical facies analysis, multivariate statistics, water quality indices, and geospatial mapping, provides complementary lines of evidence for identifying contamination patterns and the processes influencing groundwater chemistry, thereby supporting more informed groundwater assessment and environmental management in petroleum-producing sedimentary environments.

Keywords: groundwater contamination; hydrogeochemical facies; petroleum environmental engineering; Niger Delta; principal component analysis; water quality index; geospatial pollution mapping.

INTRODUCTION

Groundwater constitutes the world's largest reservoir of accessible freshwater, stored within porous and permeable geological formations and serving as the primary water source for over 2 billion people globally (WHO, 2011). It accounts for approximately 70% of global freshwater withdrawals, with agricultural, domestic, and industrial applications collectively representing 87%, 10%, and 3% of total usage, respectively (FAO, 2020). In petroleum-producing regions, this critical resource faces increasingly unprecedented threats from exploration and production activities that introduce complex mixtures of hydrocarbons, brines, heavy metals, and chemical additives into vulnerable subsurface environments (Sam et al., 2017; Ordinioha & Brisibe, 2013).

The Niger Delta of Nigeria epitomises this environmental challenge at an extreme scale. Spanning approximately 70,000 km² across nine states in southern Nigeria, this region constitutes Africa's largest wetland ecosystem and one of the world's most prolific hydrocarbon provinces (Onyena & Sam, 2020). Since the commencement of commercial oil production in 1956, the region has witnessed over 6,817 documented spill incidents between 1976 and 2001, releasing more than 3 million barrels of crude oil into the environment (United Nations Development Programme [UNDP], 2006). Contemporary estimates indicate that approximately 240,000 barrels are spilled annually, with contamination permeating surface water, groundwater, soil, and the atmosphere (Ewim et al., 2023; Ordinioha & Brisibe, 2013). The landmark United Nations Environment Programme assessment of Ogoniland (United

Nations Environment Programme [UNEP], 2011) documented extensive soil and groundwater contamination and estimated that remediation could require more than 30 years, signifying one of the most protracted environmental engineering challenges on the continent.

Hydrogeochemical investigations provide fundamental insights into groundwater quality, geochemical evolution, and potential contamination mechanisms. Graphical classification tools, notably Piper trilinear diagrams (Piper, 1944), Stiff pattern diagrams (Stiff, 1951), and expanded Durov diagrams (Durov, 1948), enable systematic characterisation of dominant water types and identification of key geochemical processes controlling groundwater composition. When integrated with multivariate statistical techniques, particularly Principal Component Analysis (PCA) and Hierarchical Cluster Analysis (HCA), these approaches offer powerful source-apportionment capabilities (Taşan et al., 2022; Gautam et al., 2024). Water quality indices, specifically the Metal Index (MI) and the Water Quality Index (WQI) translate complex multi-parameter datasets into single, policy-relevant numbers conveying contamination severity and suitability for use (Horton, 1965; Edet & Offiong, 2002). Geographic Information System (GIS) integration further enables spatial interpolation of point-source data into continuous contamination maps supporting remediation planning and environmental monitoring network design (Hamma et al., 2024; Gad et al., 2023).

Despite extensive research on Niger Delta environmental degradation, significant knowledge gaps persist concerning offshore groundwater quality dynamics. Previous hydrogeochemical studies have predominantly addressed onshore communities and coastal environments (Akakuru et al., 2021), with negligible attention to the offshore depobelts where petroleum infrastructure is most densely concentrated. Furthermore, while individual assessment methods have been applied in isolation, few investigations have employed fully integrated analytical frameworks combining all complementary techniques within a single study, limiting source attribution confidence and mechanistic understanding.

Research gap

Despite numerous investigations into groundwater quality in petroleum-producing regions, important scientific uncertainties remain regarding the dominant processes governing groundwater chemistry in offshore petroleum-producing aquifers. Existing studies have largely employed hydrogeochemical facies analysis, multivariate statistical techniques, water quality indices, or geospatial analysis as independent approaches. Consequently, it remains uncertain whether these analytical methods provide consistent and complementary evidence for identifying the relative contributions of natural hydrogeochemical processes and petroleum-related anthropogenic activities to groundwater quality deterioration. This unresolved issue limits confidence in contamination source attribution, hydrogeochemical interpretation, and the development of effective groundwater monitoring and environmental management strategies in offshore petroleum-producing environments.

Study objectives

To address this knowledge gap, the present study aims to conduct an integrated hydrogeochemical and environmental assessment of groundwater quality in an offshore petroleum-producing field of the Niger Delta depobelt. Specifically, the study seeks to (i) evaluate the physicochemical characteristics and groundwater quality status; (ii) characterise hydrogeochemical facies and the geochemical processes governing groundwater evolution; (iii) identify the dominant natural and anthropogenic factors influencing groundwater chemistry using multivariate statistical techniques; (iv) assess groundwater quality using established water quality indices; (v) investigate the spatial distribution of groundwater quality parameters and contamination patterns using GIS-based mapping; (vi) integrate hydrogeochemical, statistical, water quality index, and geospatial analyses to provide a more comprehensive understanding of the processes controlling groundwater chemistry in offshore petroleum-producing sedimentary environments.

The study is based on the hypothesis that petroleum production activities constitute a significant anthropogenic influence on groundwater hydrochemistry in the offshore Niger Delta depobelt and that the integration of hydrogeochemical facies analysis, multivariate statistical techniques, water quality indices, and GIS-based spatial analysis will provide convergent and more reliable evidence for identifying groundwater quality patterns, contamination sources, and the dominant processes controlling groundwater chemistry than the application of individual analytical methods alone.

MATERIALS AND METHODS

Study area

Location and setting

Field X is located within the offshore depobelt of the Niger Delta, a tectonically complex Tertiary sedimentary basin formed through progradation of the Niger River system over the past 66 million years (Evamy et al., 1978). The study area lies between latitudes 4°50′52"N and 4°59′6"N, and longitudes 5°33′13"E and 5°41′66"E, covering approximately 150 km² (Figure 1). The depobelt is characterised by extensive petroleum infrastructure, production platforms, subsea pipelines, wellheads, and processing facilities, representing decades of intensive hydrocarbon exploration and production, rendering it acutely vulnerable to oil spills, produced water discharges, and infrastructure-related contamination pathways that may impact groundwater quality (Figure 2).

Geological and hydrogeological setting

The Niger Delta stratigraphy comprises three major lithostratigraphic formations. The Akata Formation (Paleocene–Recent) consists of dark grey, silty pro-delta marine shales with occasional thin sand intercalations, deposited under reducing conditions and serving as the primary source rock. The Agbada Formation (Eocene–Recent) constitutes alternating paralic sands and shales deposited in delta-front and fluvial-deltaic environments, functioning as the principal petroleum reservoir in the basin. The Benin Formation (Miocene–Recent) represents the uppermost unit, coarse to medium-grained, friable continental sands characterised by high porosity (30–40%) and permeability (1,000–10,000 mD), which forms the primary aquifer system exploited for groundwater in the region (Short & Stauble, 1967; Weber & Daukoru, 1975).

The hydrogeological framework is controlled by this lithostratigraphic succession. Groundwater occurs under unconfined to semi-confined conditions depending on clay lens continuity within the Benin Formation. The water table ranges from near-surface (<1 m) along the Atlantic coastline to approximately 15 m below ground surface inland, exhibiting semi-diurnal tidal fluctuations in coastal zones and seasonal variation linked to the monsoonal rainfall pattern (April–October; 2,500–4,000 mm annually). Groundwater flow is generally oriented northeast to southwest toward the ocean. The shallow, sandy character of these coastal aquifers renders them particularly susceptible to rapid infiltration and transport of petroleum-related contaminants from surface spills and produced water discharges.

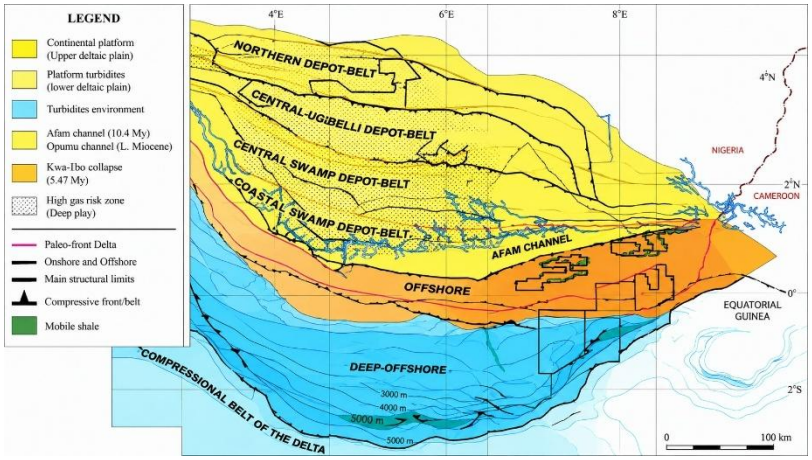

Figure 1. Location map of Field X within the offshore depobelt of the Niger Delta Basin, showing the study area extent (yellow polygon), state boundaries, and the Niger Delta regional context. Coordinates in WGS 84 (EPSG:4326)

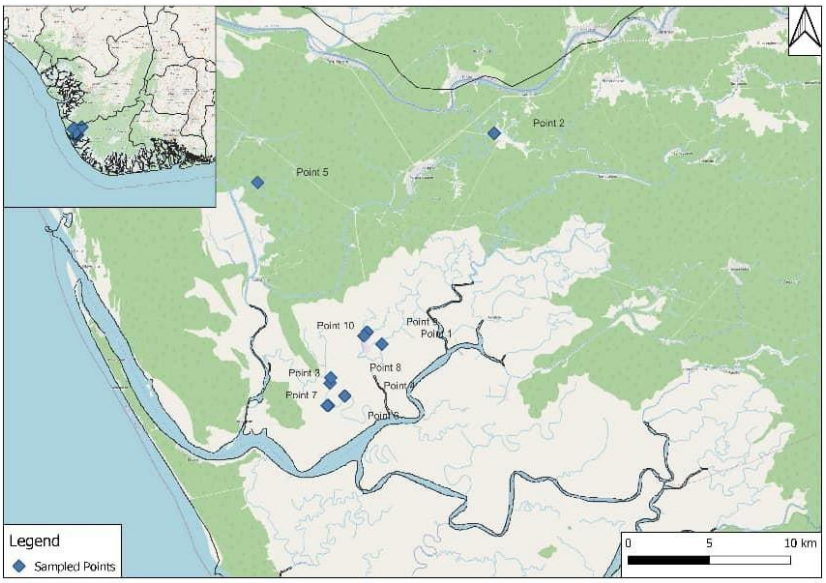

Figure 2. Detailed map of Field X showing ten groundwater sampling locations (GW1–GW10), petroleum infrastructure overlay (platforms, pipeline corridors, wellheads, storage facilities), and distance buffers at 500 m, 1,000 m, and 1,500 m from infrastructure. Base map from QGIS OpenStreetMap layer; sample points projected in UTM Zone 31N (EPSG:32631)

Sampling design and collection

A systematic sampling campaign was conducted during the dry season (January 2024) to minimise rainfall-driven dilution effects. Ten groundwater monitoring wells across Field X were selected based on their hydrogeological significance and varying proximity to petroleum infrastructure, ensuring representative spatial coverage of the study area (Table 1). The number of sampling wells was constrained by the availability of operational groundwater monitoring wells within the offshore production field. The selected wells represent the major hydrogeological sectors and encompass a gradient of distances from petroleum infrastructure, thereby providing adequate spatial coverage of the principal environmental conditions and hydrogeological settings present within the study area.

Sample coordinates were recorded using a Garmin eTrex 30x GPS device (±3–5 m horizontal accuracy). Prior to collection, each well was purged for 15–20 minutes until field parameters (pH, EC, temperature) stabilised within ±5% over three successive 5-minute readings, ensuring representative formation water rather than stagnant wellbore water was sampled.

Samples were collected in pre-cleaned 1-litre acid-washed high-density polyethylene (HDPE) bottles (rinsed three times with well water before filling). Samples for cation and heavy metal analysis were immediately acidified to pH < 2 with ultra-pure trace-metal grade HNO_3 to prevent precipitation and adsorption. Separate unacidified aliquots were collected for anion analysis. All samples were carefully placed in ice-filled coolers and transported to the laboratory within 24 hours, maintaining a controlled temperature of 4°C ± 2°C throughout transit and handling (Barcelona et al., 1985).

In-situ measurements and field QA/QC

In-situ measurements of pH, temperature, and electrical conductivity (EC) were performed using a Hach HQ40d multiparameter probe calibrated daily with certified NIST-traceable buffer solutions (pH 4.01, 7.00, 10.01) and conductivity standards (84 µS/cm and 1,413 µS/cm at 25°C). Stabilisation criteria required three consecutive readings within ±0.1 pH units, ±0.2°C, and ±5% for conductivity before recording final values. Field blanks (deionised water) and equipment rinsate blanks were analysed at each site to verify absence of cross-contamination.

Table 1. Sampling locations and geographic coordinates in Field X, Niger Delta

Sample ID	Location description	Latitude, N	Longitude, E	Distance to infrastructure, m	Infrastructure type
GW1	Northern sector	4°58′24"	5°38′42"	800	Platform A
GW2	Central, Pipeline junction	4°56′18"	5°39′15"	250	Pipeline junction
GW3	Eastern sector	4°55′36"	5°40′28"	420	Platform B
GW4	Western sector	4°57′42"	5°36′54"	950	Wellhead cluster
GW5	Southern sector	4°52′48"	5°37′36"	1,650	Remote
GW6	Central-east	4°56′54"	5°39′48"	380	Storage facility
GW7	Northwest sector	4°58′12"	5°35′24"	720	Platform C
GW8	Southeast sector	4°53′30"	5°40′12"	1,420	Remote
GW9	Northeast sector	4°57′48"	5°41′06"	560	Disposal site
GW10	Central-west	4°55′12"	5°37′18"	310	Pipeline corridor

Laboratory analysis

All analyses were conducted at Dukoria International Limited, an ISO 17025-accredited analytical laboratory, following American Public Health Association (American Public Health Association [APHA], 2017) Standard Methods for the Examination of Water and Wastewater (APHA, 2017) and ASTM protocols. All analyses commenced within 24–48 hours of sample collection.

Total Hardness was determined by EDTA complexometric titration (APHA Method 2340C). Nitrate was analysed by automated cadmium reduction with colorimetric detection at 543 nm (APHA Method 4500-NO_3^- E). Phosphate was measured using ascorbic acid reduction of molybdenum blue at 880 nm (APHA Method 4500-P E). Chloride was determined by argentometric titration (APHA Method 4500-Cl^- B). Sulphate was quantified turbidimetrically with barium chloride at 420 nm (APHA Method 4500-SO_4^{2-} E). Heavy metals (Fe, Zn, Cu, Cr, Ca, Mg, Na, K) were determined by Flame Atomic Absorption Spectrophotometry (FAAS; PerkinElmer AAnalyst 400) following EPA Method 3010A acid digestion. Total Hydrocarbon Content (THC) was extracted with n-hexane and quantified by GC-FID (Agilent 7890B). Total Suspended Solids (TSS) were measured gravimetrically using glass fibre filters (Whatman GF/C, 1.2 µm; APHA Method 2540D). Alkalinity was determined by potentiometric titration (APHA Method 2320B).

Quality control and assurance

Rigorous quality assurance and quality control (QA/QC) procedures were implemented throughout the analytical process. Reagent blanks, field blanks, duplicate samples (10% of the total samples), and certified reference materials (NIST Standard Reference Materials) were included in each analytical batch to evaluate analytical precision and accuracy. Instrument calibration was performed using a minimum of five calibration standards, with coefficients of determination (R^2) greater than 0.995 for all analytes.

Analytical precision, assessed using duplicate analyses, was consistently maintained within ±5% for major ions and ±10% for trace metals. Analytical accuracy was further verified using certified reference materials, with recoveries ranging from 95–105% for major ions and 90–110% for trace metals, confirming the reliability and reproducibility of the analytical results. Method detection limits were established and verified in accordance with the procedures outlined in EPA 40 CFR Part 136, Appendix B.

Charge balance errors (CBE) were calculated using the equation:

$$\%\ \text{Error} = \frac{\Sigma\ \text{Cations} - \Sigma\ \text{Anions}}{\Sigma\ \text{Cations} + \Sigma\ \text{Anions}} \times 100, \quad (1)$$

Approximately 90% of the groundwater samples exhibited ionic balance errors within ±5%, indicating excellent analytical consistency. The remaining samples showed charge balance errors between ±5% and ±10%, which are generally considered acceptable for natural groundwater analyses and may reflect the influence of minor unmeasured ionic constituents or inherent analytical uncertainty rather than significant analytical error. None of the samples exceeded the commonly accepted ±10% charge balance criterion; therefore, all samples were retained for subsequent hydrogeochemical interpretation.

The analytical laboratory did not report expanded measurement uncertainty for individual parameters. Nevertheless, data quality was evaluated through the combined application of calibration verification, duplicate analyses, blank analyses, certified reference materials, and ionic charge balance assessment, consistent with established hydrochemical quality assurance practices.

Hydrogeochemical facies analysis

Hydrogeochemical facies were classified using three complementary graphical methods. Major ion concentrations were converted to milliequivalent percentages (meq%) and plotted on Piper trilinear diagrams to determine dominant water types (Piper, 1944). Stiff diagrams were constructed by plotting cation and anion concentrations (meq/L) on logarithmic horizontal axes to create characteristic polygonal chemical fingerprints (Stiff, 1951). Expanded Durov diagrams incorporated pH and TDS as additional classification parameters to identify hydrogeochemical evolution pathways (Durov, 1948). All hydrogeochemical diagrams were generated using AqQA Geochemistry Software (RockWare, Inc., Golden, Colorado, USA). The software version was not recorded during analysis.

Multivariate statistical analysis

Prior to correlation analysis, the normality of each hydrochemical variable was assessed using the Shapiro–Wilk test together with visual inspection of Q–Q plots. The variables were found to be approximately normally distributed ($p > 0.05$), supporting the use of Pearson's correlation coefficient. Pearson correlation analysis was subsequently performed to quantify linear relationships between pairs of hydrochemical parameters using a two-tailed significance level of $p < 0.05$.

Principal component analysis (PCA) was performed on z-score-normalised data using IBM SPSS Statistics v26.0 to identify the principal factors controlling the hydrochemical characteristics of the groundwater. Components were retained based on Kaiser's criterion (eigenvalue > 1.0) and a cumulative variance threshold of >70%. Varimax orthogonal rotation was applied to facilitate interpretation of the extracted components. Factor loadings were classified as strong (|r| > 0.7), moderate (0.5–0.7), or weak (<0.5), following Liu et al. (2003).

Hierarchical cluster analysis (HCA) was performed to group groundwater sampling locations according to similarities in their hydrochemical characteristics. The analysis was conducted using the Unweighted Pair Group Method with Arithmetic Mean (UPGMA) and Euclidean distance as the similarity measure. The optimal number of clusters was determined from the hierarchical structure of the resulting dendrogram. HCA was performed using PAST v4.03 (Hammer et al., 2001), while PCA and Pearson correlation analysis were conducted using IBM SPSS Statistics v26.0.

Water quality index calculations

The metal index (MI) was calculated to assess the overall degree of heavy-metal contamination in groundwater following the approach proposed by Edet & Offiong (2002). The MI was calculated as:

$$MI = \sum \frac{C_i}{MAC_I}, \quad (2)$$

where C_i is the measured concentration of the i-th metal, MAC_i is the corresponding maximum admissible concentration, and n is the number of metals included in the assessment. The analysis included Fe, Zn, Cu, and Cr. The applicable maximum admissible concentrations were obtained from the World Health Organization (WHO) drinking-water guidelines and the relevant Nigerian regulatory standards. The calculated MI values were interpreted according to the classification scheme adopted for this study (Table 2).

The water quality index (WQI) was calculated using Horton's weighted arithmetic index method (Horton, 1965) to assess the overall suitability of groundwater for domestic use. The quality rating for each parameter was calculated as:

$$q_n = \frac{V_n - V_i}{S_n - V_i} \times 100, \quad (3)$$

where V_n is the observed concentration of the parameter, V_i is the ideal value in pure water (7.0 for pH and 0 for all other parameters), and S_n is the corresponding drinking-water standard.

The unit weight for each parameter was calculated as:

$$W_n = \frac{k}{S_n}, \quad (4)$$

where $k = \frac{1}{\sum(1/S_n)}$.

The overall WQI was calculated as:

$$WQI = \frac{\sum(q_n W_n)}{\sum W_n}. \quad (5)$$

The WQI incorporated the physicochemical parameters selected for drinking-water quality assessment. WQI values were classified as excellent (<25), good (25–50), poor (50–75), very poor (75–100), and unsuitable (>100) as summarised in Table 3.

Table 2. MI classification scheme and water quality status

MI range	Class	Water quality status
< 0.3	I	Pure water
0.3–1.0	II	Slightly affected
1.0–2.0	III	Moderately affected
2.0–4.0	IV	Significantly affected
4.0–6.0	V	Seriously affected
> 6.0	VI	Unsuitable for consumption

Table 3. WQI classification and usage recommendations

WQI range	Water quality	Recommended use
< 25	Excellent	Drinking, domestic, irrigation, industrial
25–50	Good	Drinking, domestic, irrigation
50–75	Poor	Irrigation and industrial only
75–100	Very poor	Irrigation with treatment
> 100	Unsuitable	Treatment required before any use

Geospatial analysis

Spatial distribution maps were generated in QGIS v3.28 "Firenze". Sample coordinates were imported in WGS 84 (EPSG:4326) and projected to UTM Zone 31N (EPSG:32631). IDW interpolation was applied using the formula:

$$Z = \frac{\sum(z_i/d_i^p)}{\sum(1/d_i^p)}, \quad (6)$$

where power parameter p = 2, variable search radius with 12 nearest neighbours, and 100 m output cell size (Shepard, 1968). Maps were classified using natural breaks (Jenks) and overlaid with petroleum infrastructure layers to explore potential spatial relationships between hydrochemical parameters and proximity to petroleum infrastructure. The interpolated maps were intended to illustrate spatial trends rather than provide high-resolution prediction surfaces, because

of the limited number of sampling locations available for interpolation.

Limitations of the study

Several important limitations should be carefully considered when interpreting the findings and conclusions of this study. First, only ten operational groundwater monitoring wells were available within the offshore production field, which constrains the statistical power of the principal component analysis, hierarchical cluster analysis, and spatial interpolation, and limits the broader generalisation of the results. Second, sampling was conducted during a single dry-season campaign and therefore represents a spatial snapshot of groundwater conditions rather than fully capturing temporal, seasonal, or short-term variability in groundwater quality across the study area. Third, the IDW interpolation surfaces should be interpreted as illustrations of spatial trends rather than precise, high-resolution prediction surfaces, given the limited number of sampling locations. Fourth, PCA and HCA are exploratory pattern-recognition techniques that identify covariance structures and similarities among samples; they provide statistically supported associations rather than direct, causal evidence of contamination sources. These limitations do not invalidate the findings but indicate that conclusions regarding petroleum-related influences on groundwater quality should be regarded as evidence-based and consistent with the available data, rather than definitive, while acknowledging the inherent uncertainties associated with the current dataset. Future studies incorporating larger monitoring networks, multi-season sampling, and longer-term temporal observations are therefore warranted to further validate these findings.

RESULTS

Overview of groundwater chemistry

The physicochemical characteristics and chemical composition of groundwater samples from Field X are summarized in Tables 4–6. Tables 4 and 5 present the analytical results for major physicochemical parameters, major ions, and trace metals, whereas Table 6 summarizes the descriptive statistics of selected variables. Comparison with WHO (2017) guideline values indicates that several parameters, including EC, TDS, TSS, Mg^{2+}, SO_4^{2-}, Fe, and Cr^{6+}, exceeded the recommended limits in a substantial proportion of samples, highlighting widespread departures from established drinking-water quality standards across the study area.

Table 4. Physicochemical parameters and major cation concentrations in groundwater samples from Field X (WHO guideline values in bold)

Sample	pH	T, °C	EC, µS/cm	TDS, mg/L	Ca^{2+}, mg/L	Mg^{2+}, mg/L	Na^{+}, mg/L	K^{+}, mg/L	Alk, mg/L
GW1	7.2	28.4	1,245	1,582	88.4	132.6	165.2	12.4	285
GW2	6.8	29.1	1,842	2,338	118.6	210.4	245.8	18.6	342
GW3	7.4	27.8	1,386	1,758	94.2	156.8	188.4	14.2	298
GW4	6.9	28.9	1,624	2,062	108.4	178.2	218.6	16.8	325
GW5	7.6	27.2	918	1,165	72.6	98.4	124.2	9.2	245
GW6	7.1	28.5	1,452	1,845	96.8	162.4	192.6	14.8	305
GW7	6.7	29.4	1,585	2,014	104.2	172.6	208.4	15.9	318
GW8	7.8	26.8	852	1,082	68.4	102.2	118.6	8.6	228
GW9	7.3	27.6	1,118	1,422	82.6	125.4	148.2	11.2	268
GW10	6.6	29.8	1,728	2,196	112.8	196.2	232.4	17.4	348
WHO	**6.5–8.5**	**–**	**500**	**1,000**	**75**	**50**	**200**	**12**	**200**

Table 5. Anion and trace metal concentrations in groundwater samples from Field X (mg/L) (WHO guideline values in bold)

Sample	Cl^{-}	SO_4^{2-}	NO_3^{-}	PO_4^{3-}	TSS	Fe	Zn	Cu	Cr^{6+}
GW1	245	342	8.4	2.1	265	4.82	2.38	0.52	0.034
GW2	398	548	14.2	4.8	520	12.45	5.82	1.24	0.082
GW3	278	386	9.8	2.6	312	5.64	2.84	0.64	0.042
GW4	342	465	12.4	3.8	445	8.26	4.18	0.96	0.068
GW5	186	210	5.2	1.4	145	2.84	1.22	0.28	0.018
GW6	288	398	10.2	2.8	328	6.24	3.16	0.72	0.048
GW7	358	485	13.8	4.2	398	9.62	4.58	1.08	0.074
GW8	172	245	4.8	1.2	168	3.18	1.42	0.32	0.022
GW9	224	620	6.8	8.4	225	4.26	1.84	0.42	0.028
GW10	382	528	15.6	5.2	485	11.82	5.42	1.18	0.078
WHO	**250**	**250**	**50**	**5.0**	**25**	**0.3**	**3.0**	**2.0**	**0.05**

Table 6. Statistical summary of selected physicochemical parameters for groundwater samples

Parameter	Min	Max	Mean	Median	SD	CV%	Skewness	WHO limit
pH	6.6	7.8	7.18	7.20	0.38	5.3	−0.12	6.5–8.5
EC, µS/cm	852	1,842	1,375	1,419	323	23.5	0.24	500
TDS, mg/L	1,082	2,338	1,746	1,802	410	23.5	0.24	1,000
TSS, mg/L	145	520	329	320	121	36.8	0.42	25
Fe, mg/L	2.84	12.45	6.91	6.44	3.18	46.0	0.58	0.3
Zn, mg/L	1.22	5.82	3.29	2.97	1.52	46.2	0.55	3.0
SO_4^{2-}, mg/L	210	620	385	436	129	33.5	0.46	250
Mg^{2+}, mg/L	98	210	145	154	36.4	25.1	0.34	50

Hydrogeochemical facies classification

Piper diagram analysis revealed that all ten groundwater samples plot within the Magnesium-Sulphate (Mg-SO_4) field, identifying this as the dominant hydrogeochemical water type across Field X (Figure 3). Mg^{2+} (mean: 145 mg/L; range: 98–210 mg/L) and SO_4^{2-} (mean: 385 mg/L; range: 210–620 mg/L) dominated cation and anion chemistry, respectively, far exceeding WHO guidelines (Mg^{2+}: 50 mg/L; SO_4^{2-}: 250 mg/L). This facies is characteristic of groundwater influenced by petroleum brine mixing and sulphate enrichment from hydrocarbon operations. The Durov diagram confirmed Mg-SO_4 dominance and additionally identified TDS (range: 1,082–2,338 mg/L) as a major contributing parameter (Figure 4).

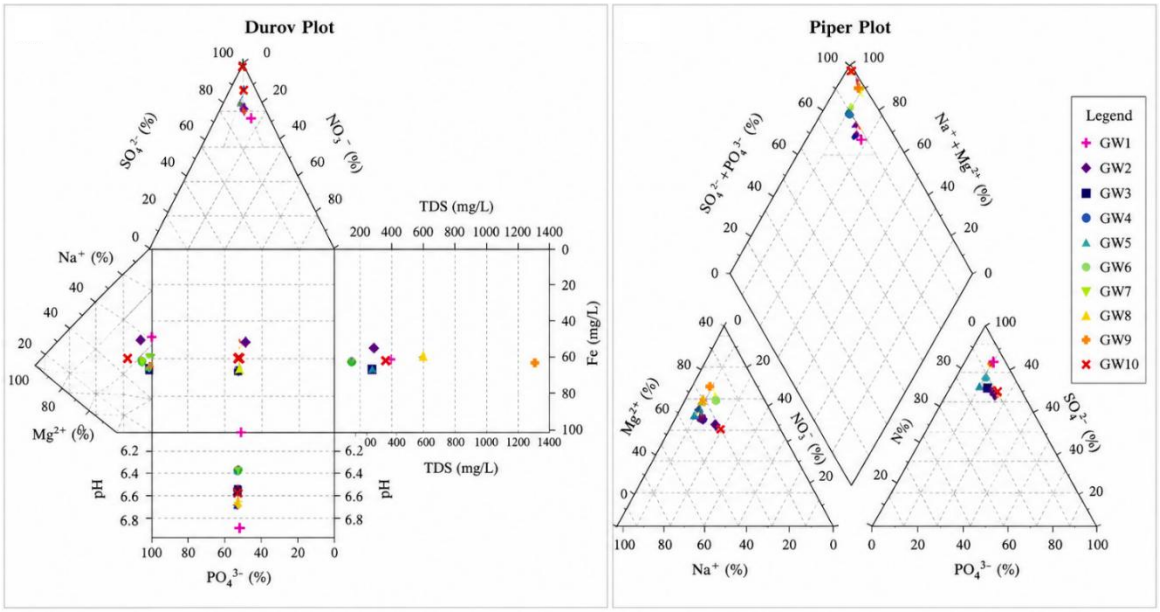

Figure 3. Piper trilinear diagram showing hydrogeochemical facies classification of groundwater samples GW1–GW10. All samples plot within the Magnesium-Sulphate (Mg-SO_4) field in the central diamond field.
The diagram was generated using AqQA v2.2 software (data derived from Tables 4 and 5)

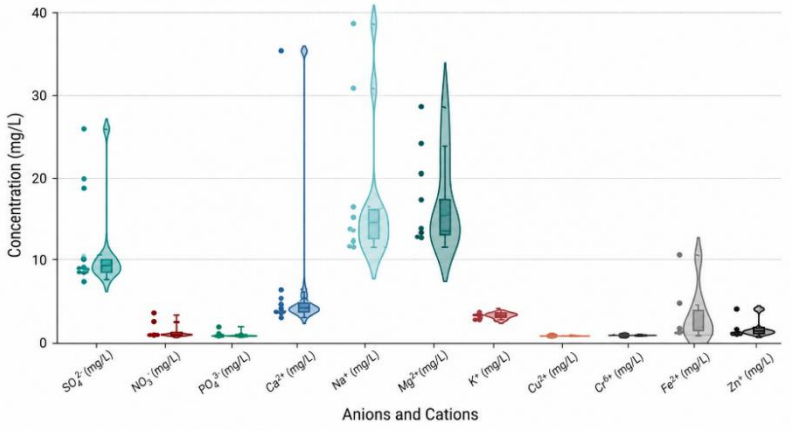

Figure 4. Expanded Durov diagram showing hydrochemical facies classification with TDS (vertical right axis) and pH (horizontal bottom axis) as additional parameters. The diagram indicates Mg-SO_4 dominance and highlights TDS as an important parameter influencing groundwater chemistry (constructed using AqQA v2.2 software)

Stiff diagrams for GW1–GW10 demonstrated notable uniformity, with extended arms on the Mg^{2+} and SO_4^{2-} axes, confirming consistency of this geochemical signature across the study area (Figures 5–9).

Stiff plot of GW1 through GW10 revealing uniformity in dominant ionic concentration, i.e. Magnesium ion and Sulphate Ion. This is in conformity with Durov and Piper plots.

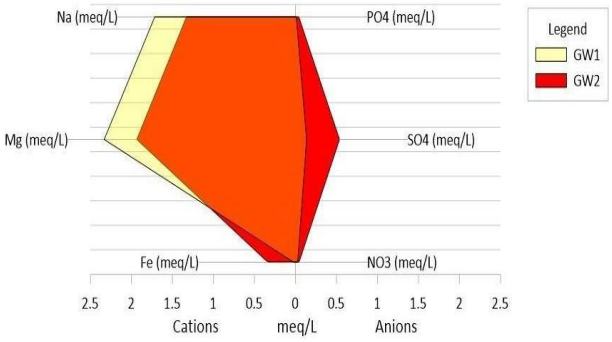

Figure 5. Stiff diagrams comparing the predominant ionic composition of groundwater samples GW1 and GW2

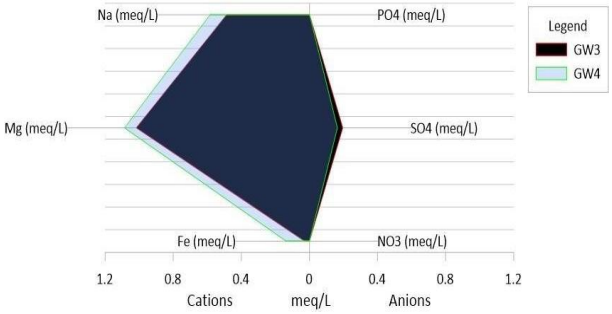

Figure 6. Stiff diagrams comparing the predominant ionic composition of groundwater samples GW2 and GW3

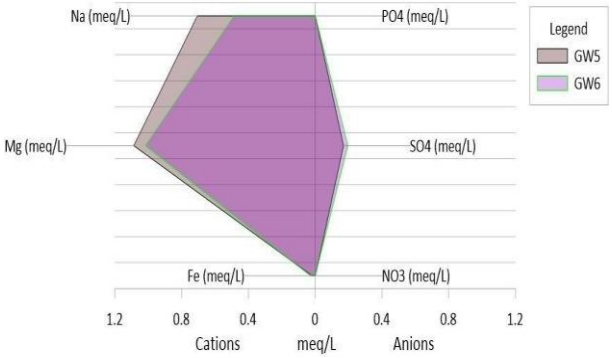

Figure 7. Stiff diagrams comparing the predominant ionic composition of groundwater samples GW5 and GW6

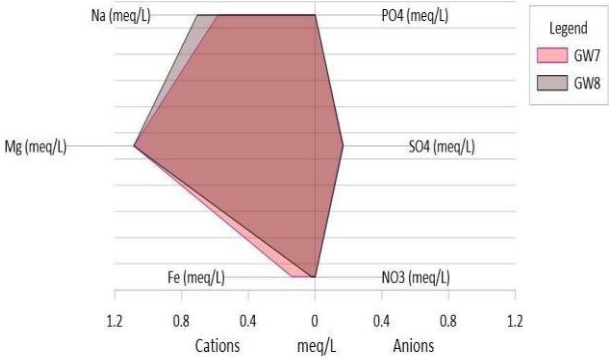

Figure 8. Stiff diagrams comparing the predominant ionic composition of groundwater samples GW7 and GW8

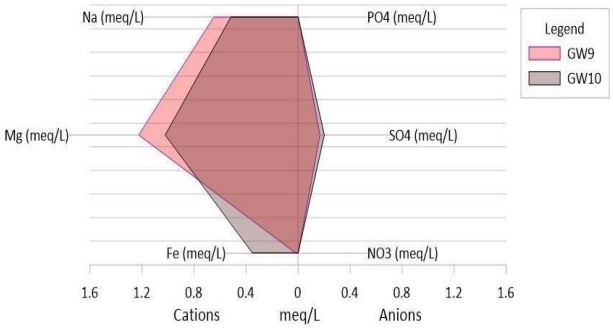

Figure 9. Stiff diagrams comparing the predominant ionic composition of groundwater samples GW9 and GW10

Pearson correlation analysis

Pearson correlation analysis revealed significant associations among hydrochemical parameters. Strong positive correlations were identified between Zn and Cu ($r = 0.712$, $p < 0.01$) and between Zn and Fe ($r = 0.685$, $p < 0.01$), suggesting common petroleum-related anthropogenic influences. Positive correlations between pH and EC ($r = 0.452$, $p < 0.05$) and between SO_4^{2-} and Mg^{2+} ($r = 0.524$, $p < 0.05$) suggest coupled geochemical processes associated with petroleum brine influence and mineral dissolution. A weak negative correlation between temperature and TSS ($r = –0.258$) may indicate limited temperature-related effects on suspended sediment dynamics in the shallow coastal aquifer.

Principal component analysis (PCA)

PCA extracted three components with eigenvalues exceeding 1.0 (Kaiser criterion), collectively accounting for 83.1% of total variance (Table 7). Component loadings following varimax rotation are presented in Table 8. PCA identifies covariance structures among the measured variables and does not, by itself, independently establish contamination sources; therefore, component interpretations presented below are considered evidence-based hypotheses that require further validation rather than definitive source attributions.

Principal component 1 (PC1)

PC1 explained 46.65% of the total variance and exhibited high positive loadings for Zn (0.882), Cu (0.845), Mg^{2+} (0.768), Na^{+} (0.724), NO_3^{-} (0.692), Fe (0.628), and K^{+} (0.586), as illustrated in Figure 10. This component was interpreted as representing a petroleum-related hydrochemical influence, reflecting the potential contribution of hydrocarbon-associated sources, including oil spills, produced water discharge, drilling fluid inputs, and infrastructure corrosion.

Principal component 2 (PC2)

PC2 explained 19.88% of the total variance and exhibited strong positive loadings for EC (0.858), TDS (0.836), and Ca^{2+} (0.732) (Figure 11). This component was labelled as the Geochemical Salinity Factor, representing natural water–rock interactions enhanced by petroleum formation brine mixing with fresh groundwater.

Principal component 3 (PC3)

PC3 explained 16.56% of the total variance and exhibited high positive loadings for SO_4^{2-} (0.794) and PO_4^{3-} (0.721), as illustrated in Figure 12. This component was interpreted as representing a Sulphate–Phosphate Enrichment This factor reflects the potential influence of petroleum brines through sulphate-enriched formation waters, together with nutrient inputs associated with petroleum-related chemical additives and production activities.

Table 7. Principal component analysis eigenvalues and variance explained

Component	Eigenvalue	Variance, %	Cumulative, %
PC1 – petroleum-associated influence	6.532	46.654	46.654
PC2 – geochemical salinity	2.783	19.882	66.536
PC3 – SO_4-PO_4 enrichment	2.319	16.558	83.094

Table 8. Rotated component matrix (Varimax rotation). Factor loadings > 0.5 indicate moderate-to-strong associations and are highlighted in bold

Parameter	PC1 (46.65%)	PC2 (19.88%)	PC3 (16.56%)
pH	0.342	0.124	−0.086
EC	0.256	**0.858**	0.168
TDS	0.248	**0.836**	0.142
TSS	0.468	−0.124	0.286
Ca^{2+}	0.412	**0.732**	0.098
Mg^{2+}	**0.768**	0.286	0.124
Na^{+}	**0.724**	0.368	0.186
K^{+}	**0.586**	0.242	0.156
Cl^{-}	0.492	0.458	0.268
SO_4^{2-}	0.386	0.198	**0.794**
NO_3^{-}	**0.692**	0.226	0.324
PO_4^{3-}	0.412	0.168	**0.721**
Fe	**0.628**	0.142	0.286
Zn	**0.882**	0.186	0.124

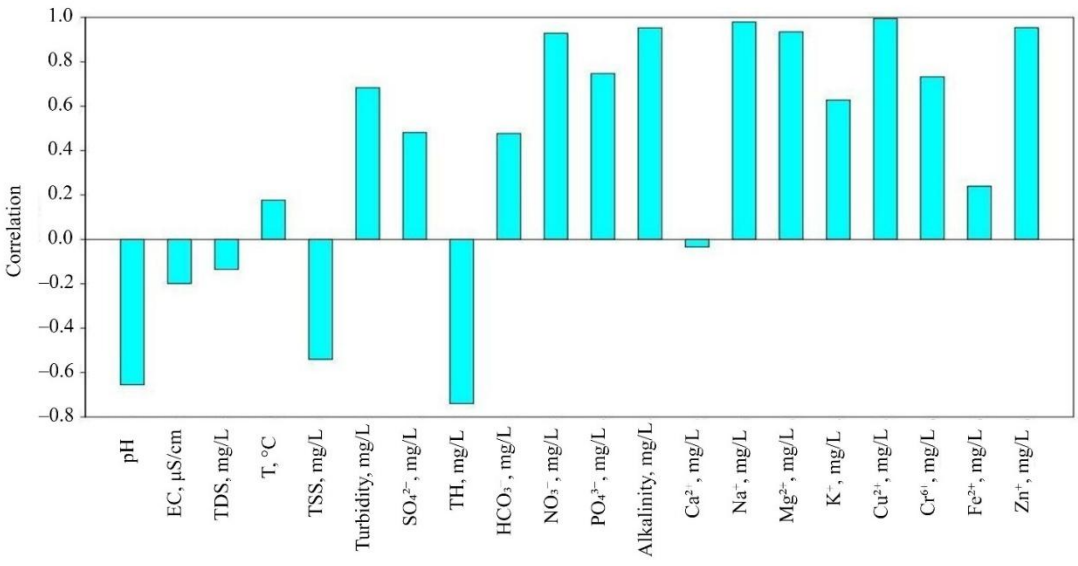

Figure 10. Relationships between PC1 scores and hydrochemical parameters

Relationships between principal components

Scatter plot analysis was performed to evaluate the relationships between the extracted principal components, as illustrated in Figure 13. The bivariate relationships between PC1 and PC2, PC2 and PC3, and PC1 and PC3 were examined to assess the distribution patterns and potential associations among the dominant hydrochemical processes identified by PCA.

Hierarchical cluster analysis (HCA)

Hierarchical cluster analysis (HCA) identified four distinct clusters among the ten groundwater sampling locations based on similarities in their hydrochemical composition (Figure 14). The identified clusters were as follows:
Cluster 1: GW1, GW4, and GW7;
Cluster 2: GW2, GW3, GW6, and GW10;
Cluster 3: GW5 and GW8;
Cluster 4: GW9.

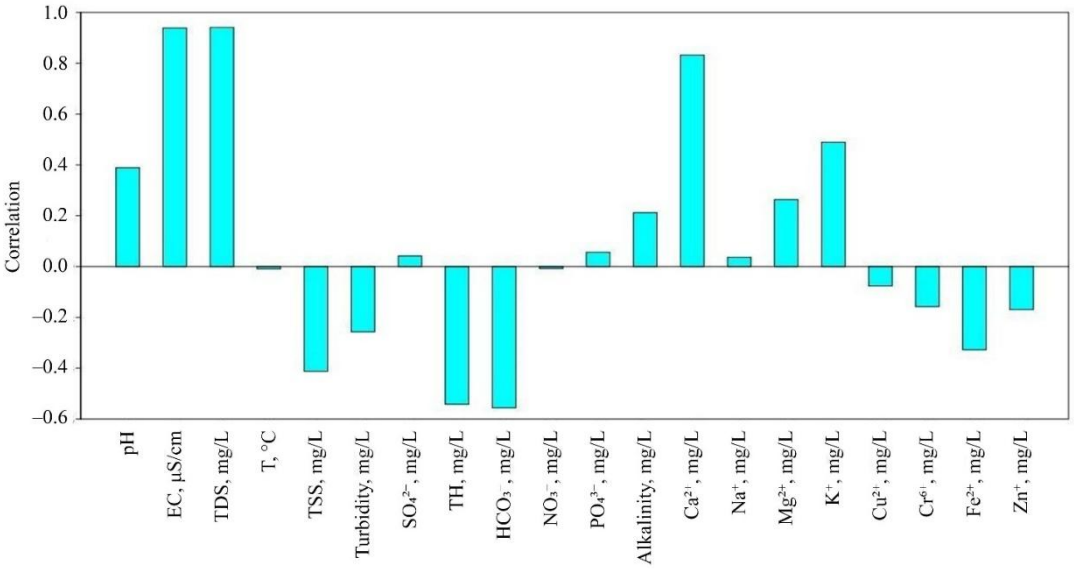

Figure 11. Relationships between PC2 scores and hydrochemical parameters

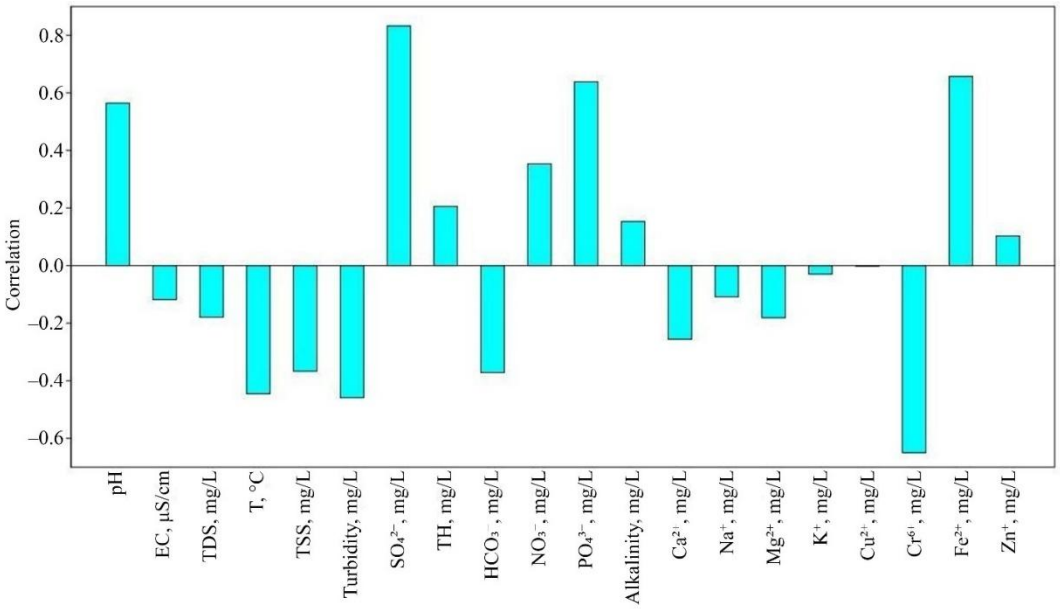

Figure 12. Relationships between PC3 scores and hydrochemical parameters

Sampling locations grouped within the same cluster exhibited similar patterns in the concentrations of the analysed chemical constituents. Cluster 2 comprised the largest number of sampling locations, whereas GW9 formed a separate cluster, indicating a comparatively distinct hydrochemical composition.

The distribution of the HCA clusters in relation to groundwater quality indices and proximity to petroleum infrastructure is presented in Table 9, providing an integrated overview of the spatial patterns and associated water-quality characteristics identified across the study area. Cluster 2, comprising GW2, GW3, GW6, and GW10, was associated with the highest Metal Index (MI) and Water Quality Index (WQI) values, ranging from 3.2 to 4.8 and from 218 to 284, respectively. These sampling locations were situated within 500 m of petroleum infrastructure. Cluster 1 (GW1, GW4, and GW7), located at distances of 500–1,000 m, showed comparatively lower MI and WQI values, ranging from 1.8 to 2.4 and from 142 to 186, respectively. Cluster 3 (GW5 and GW8), located more than 1,500 m from petroleum infrastructure, exhibited the lowest MI and WQI values, ranging from 0.9 to 1.2 and from 105 to 128, respectively.

Cluster 4 consisted solely of GW9, which was located approximately 560 m from a disposal site. This sampling location was characterised by comparatively elevated sulphate (620 mg/L) and phosphate (8.4 mg/L) concentrations, clearly distinguishing it from the other groundwater locations. The observed chemical characteristics of GW9 may indicate a localised hydrochemical influence associated with site-specific conditions; however, the HCA results alone do not establish a specific contamination source, pathway, or causal relationship.

Overall, the HCA results demonstrate distinct groupings of groundwater locations according to their hydrochemical characteristics. The observed differences in MI and WQI values among the clusters provide further evidence of variation in groundwater quality across the study area. The hierarchical relationships and cluster membership of the sampling locations are illustrated in the dendrogram (Figure 14).

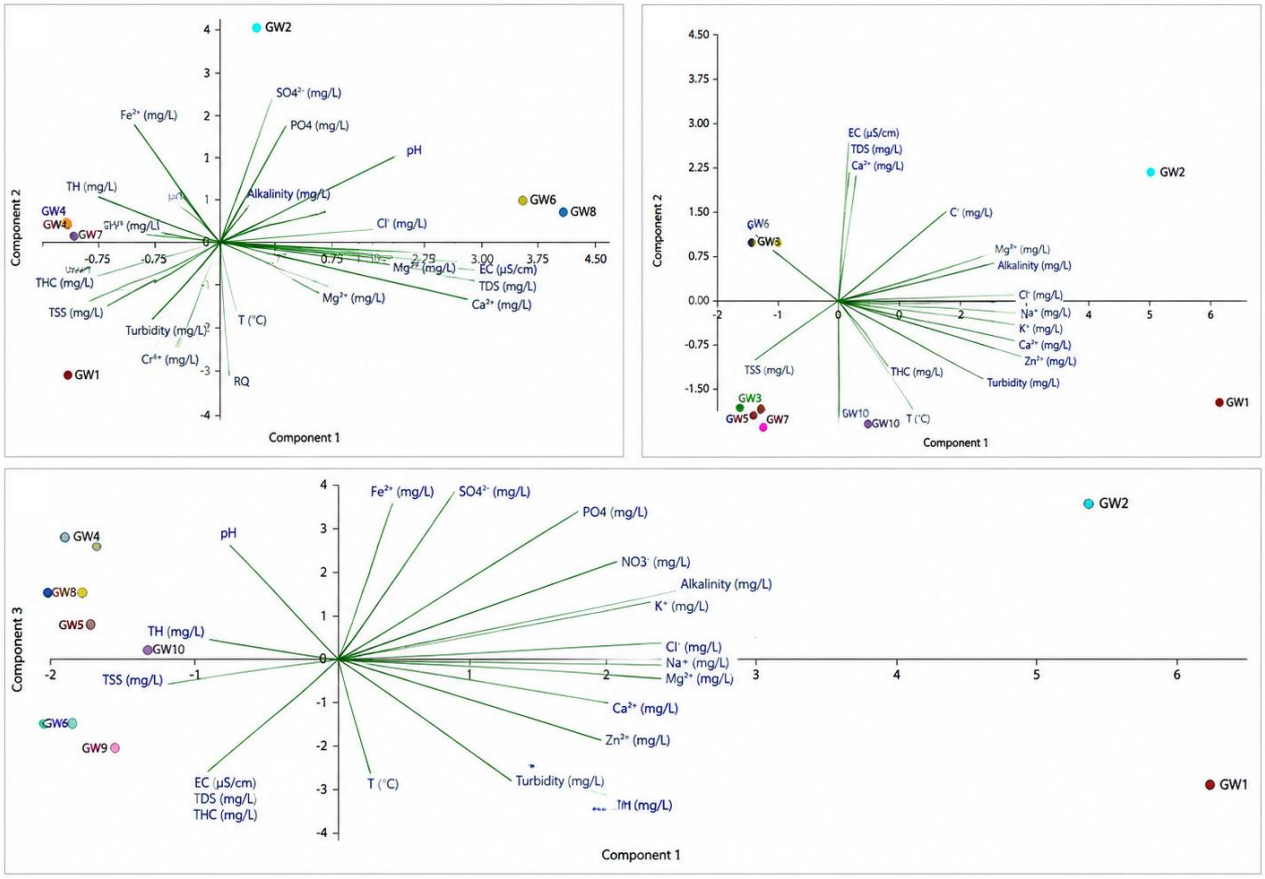

Figure 13. Pairwise relationships between PC1, PC2, and PC3 scores

Figure 14. Dendrogram obtained from hierarchical cluster analysis using the UPGMA algorithm and Euclidean distance. The four identified clusters comprise Cluster 1 (GW1, GW4, GW7), Cluster 2 (GW2, GW3, GW6, GW10), Cluster 3 (GW5, GW8), and Cluster 4 (GW9). The dendrogram illustrates the hierarchical relationships among the groundwater sampling locations based on similarities in their hydrochemical characteristics. Generated using PAST v4.03.

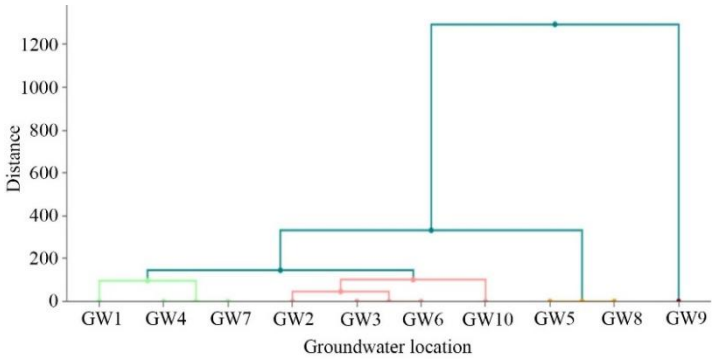

Figure 14. Hierarchical cluster analysis dendrogram showing the four clusters of groundwater sampling locations

Table 9. Hierarchical cluster composition, hydrochemical characteristics, and groundwater quality indices

Cluster	Sampling locations	MI range	WQI range	Distance, m	Groundwater quality classification	Key hydrochemical feature
1	GW1, GW4, GW7	1.8–2.4	142–186	500–1,000	Moderate (Class III–IV)	–
2	GW2, GW3, GW6, GW10	3.2–4.8	218–284	250–500	Severe (Class IV–V)	–
3	GW5, GW8	0.9–1.2	105–128	>1,400	Low (Class II–III)	–
4	GW9	1.4	164	560 (disposal site)	Moderate (Class III)	Elevated SO_4^{2-} and PO_4^{3-}

Note: Distance values represent the distance to the nearest petroleum-related facility; for GW9, the reported distance refers specifically to the nearest disposal site. MI and WQI ranges represent the minimum and maximum values within each cluster

Water quality index assessment

The metal index (MI) values presented in Table 10 ranged from 0.94 at GW5 (Class II) to 4.82 at GW2 (Class V), indicating substantial variation in the degree of metal-related groundwater quality deterioration among the sampling locations. Iron was the predominant contributor to the MI, accounting for approximately 45–60% of the index values. Fe concentrations ranged from 2.84 to 12.45 mg/L, exceeding the WHO guideline value of 0.3 mg/L by approximately 9–41-fold. Zinc represented the second-largest contribution to the MI, accounting for approximately 25–35% of the index. Zn concentrations ranged from 1.22 to 5.82 mg/L, with the maximum concentration exceeding the WHO guideline value of 3.0 mg/L by approximately 1.9-fold. Copper and chromium contributed comparatively smaller proportions to the MI, although concentrations above the applicable guideline values were observed at several sampling locations.

The water quality index (WQI) values (Table 11) ranged from 105 at GW5 to 284 at GW2. All ten groundwater sampling locations recorded WQI values above 100, corresponding to the unsuitable for drinking category according to the adopted classification scheme. Total suspended solids (TSS) represented the largest contribution to the WQI, accounting for approximately 35–55% of the index. TSS concentrations ranged from 145 to 520 mg/L, corresponding to approximately 6–21 times the adopted guideline value of 25 mg/L. Other notable contributors to the WQI were electrical conductivity (EC), which accounted for approximately 15–25%, followed by Fe (10–20%), total dissolved solids (TDS) (10–15%), and total hardness (5–10%).

Overall, the MI and WQI results indicate a consistent deterioration in groundwater quality across the study area. The highest index values were recorded at GW2, whereas GW5 exhibited the lowest MI and WQI values among the sampled locations. The predominance of Fe in the MI and TSS in the WQI highlights these parameters as the major contributors to the observed groundwater quality impairment and overall deterioration across the study area.

Table 10. Metal index (MI) component values and final classification for groundwater samples

Sample	Fe ratio	Zn ratio	Cu ratio	Cr ratio	MI value	Class
GW1	16.07	0.79	0.26	0.68	2.12	III – Moderate
GW2	41.50	1.94	0.62	1.64	4.82	V – Seriously affected
GW3	18.80	0.95	0.32	0.84	2.48	IV – Significant
GW4	27.53	1.39	0.48	1.36	3.45	IV – Significant
GW5	9.47	0.41	0.14	0.36	0.94	II – Slightly affected
GW6	20.80	1.05	0.36	0.96	2.86	IV – Significant
GW7	32.07	1.53	0.54	1.48	4.12	V – Seriously affected
GW8	10.60	0.47	0.16	0.44	1.18	III – Moderate
GW9	14.20	0.61	0.21	0.56	1.42	III – Moderate
GW10	39.40	1.81	0.59	1.56	4.58	V – Seriously affected

Table 11. Water quality index (WQI) values, quality classification, and major contributing parameters for groundwater samples

Sample	WQI	Quality classification	Primary contributor	Secondary contributor
GW1	142	Unsuitable	TSS (45%)	Fe (18%)
GW2	284	Unsuitable	TSS (52%)	Fe (22%)
GW3	168	Unsuitable	TSS (48%)	EC (16%)
GW4	216	Unsuitable	TSS (51%)	Fe (19%)
GW5	105	Unsuitable	TSS (38%)	EC (14%)
GW6	178	Unsuitable	TSS (47%)	Fe (17%)
GW7	234	Unsuitable	TSS (49%)	Fe (20%)
GW8	118	Unsuitable	TSS (42%)	EC (15%)
GW9	164	Unsuitable	TSS (44%)	SO_4^{2-} (24%)
GW10	268	Unsuitable	TSS (54%)	Fe (21%)

Note: WQI values >100 indicate water unsuitable for drinking according to the classification scheme adopted in this study. Percentages indicate the relative contribution of individual parameters to the calculated WQI

Geospatial analysis

The spatial distribution of the investigated hydrochemical parameters was evaluated using geospatial interpolation, and the resulting distribution patterns are presented in Figures 15–19. The maps demonstrate spatial heterogeneity in groundwater chemistry across the study area, with the degree and pattern of variation differing among individual parameters.

Figure 15 presents the spatial distributions of pH, sulphate, total suspended solids (TSS), and sodium. The pH distribution shows a distinct localised zone of comparatively lower pH values

in the central part of the study area, while higher values extend across the surrounding areas. Sulphate also exhibits spatial variability, with a localised area of comparatively elevated concentrations around the central group of sampling locations.

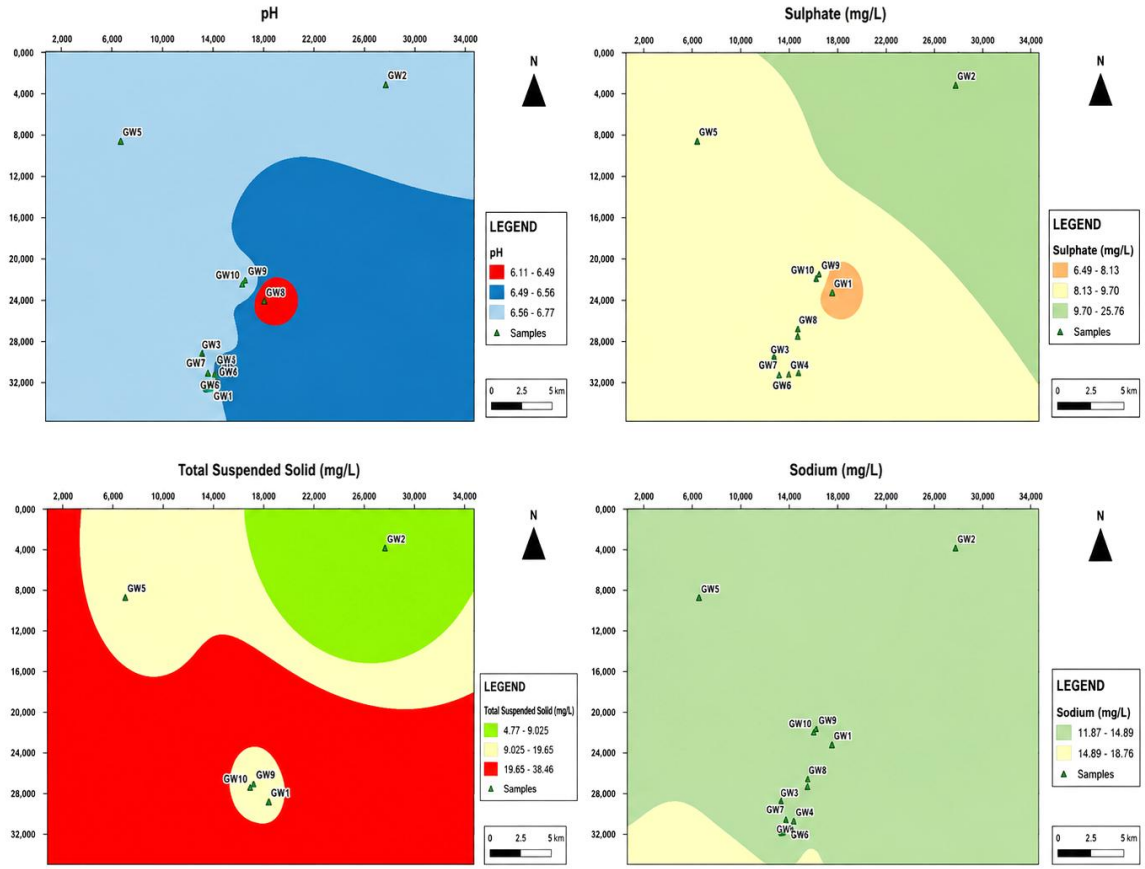

Figure 15. Spatial distribution of pH, sulphate, total suspended solids (TSS), and sodium concentrations across the study area

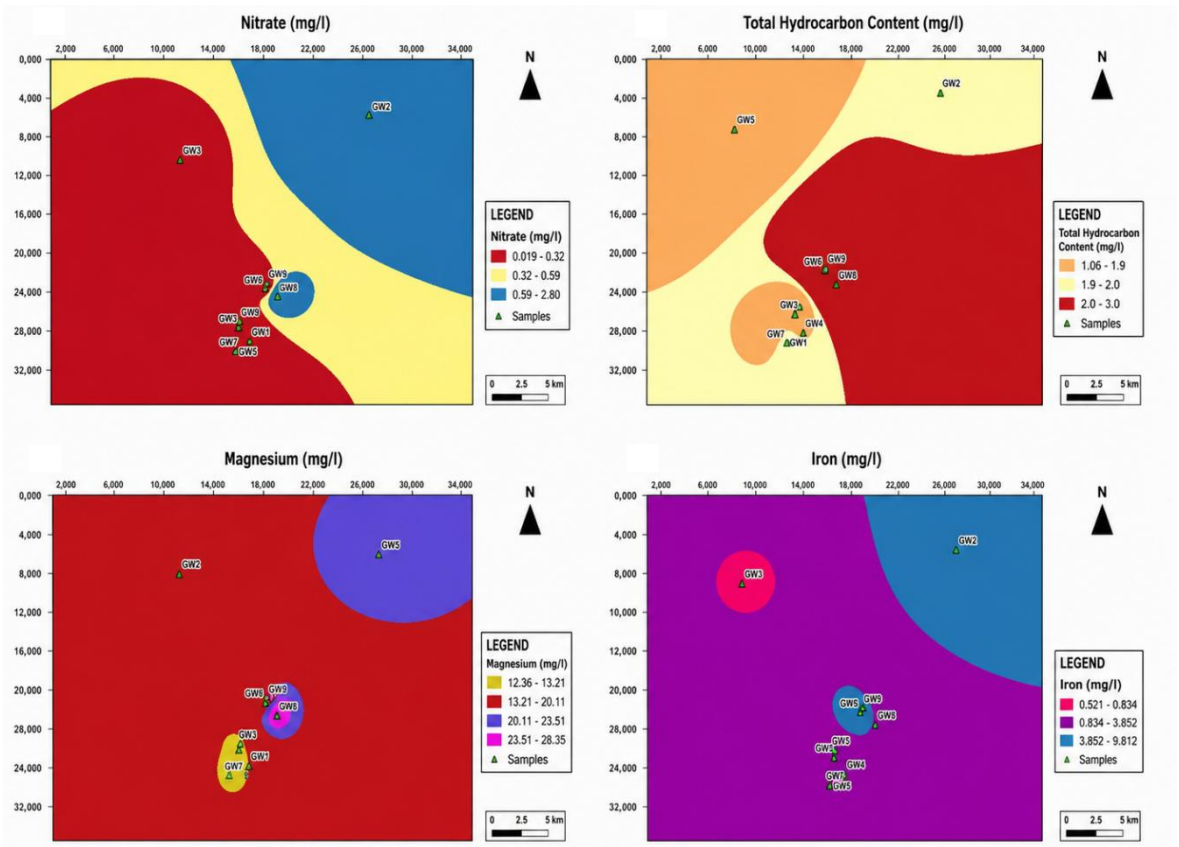

Figure 16. Spatial distribution of nitrate, magnesium, iron, and total hydrocarbon content (THC) across the study area

The distribution of TSS shows pronounced spatial heterogeneity, with higher concentrations occurring towards the southern and central portions of the mapped area and comparatively lower concentrations in the northern part. In contrast, sodium displays a comparatively broader and more uniform spatial distribution, with local variations occurring around the sampling area.

The spatial distributions of nitrate, magnesium, iron, and total hydrocarbon content (THC) are presented in Figure 16. Figure 17 shows the spatial distributions of copper, chromium, and phosphate, while Figure 18 presents the distributions of potassium, electrical conductivity (EC), zinc, and calcium. The spatial distributions of total dissolved solids (TDS) and temperature are presented in Figure 19.

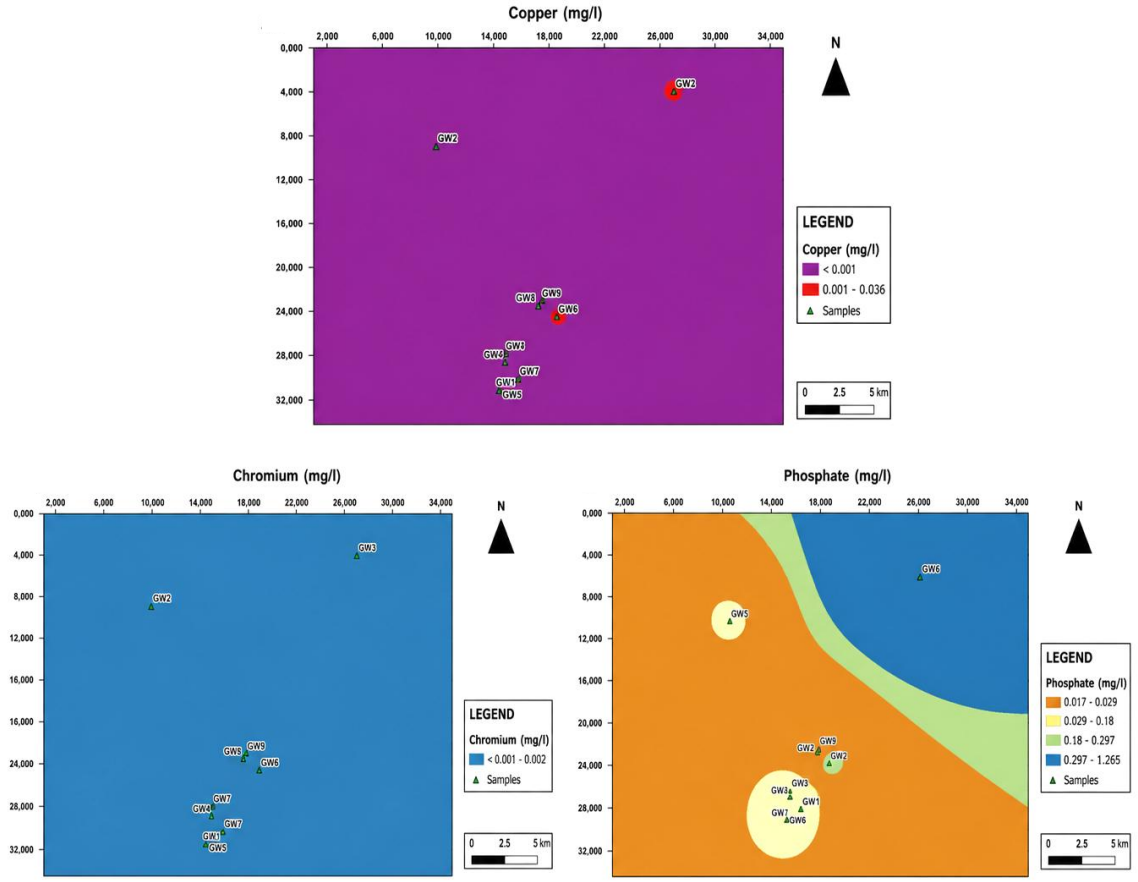

Figure 17. Spatial distribution of copper, chromium, and phosphate concentrations across the study area

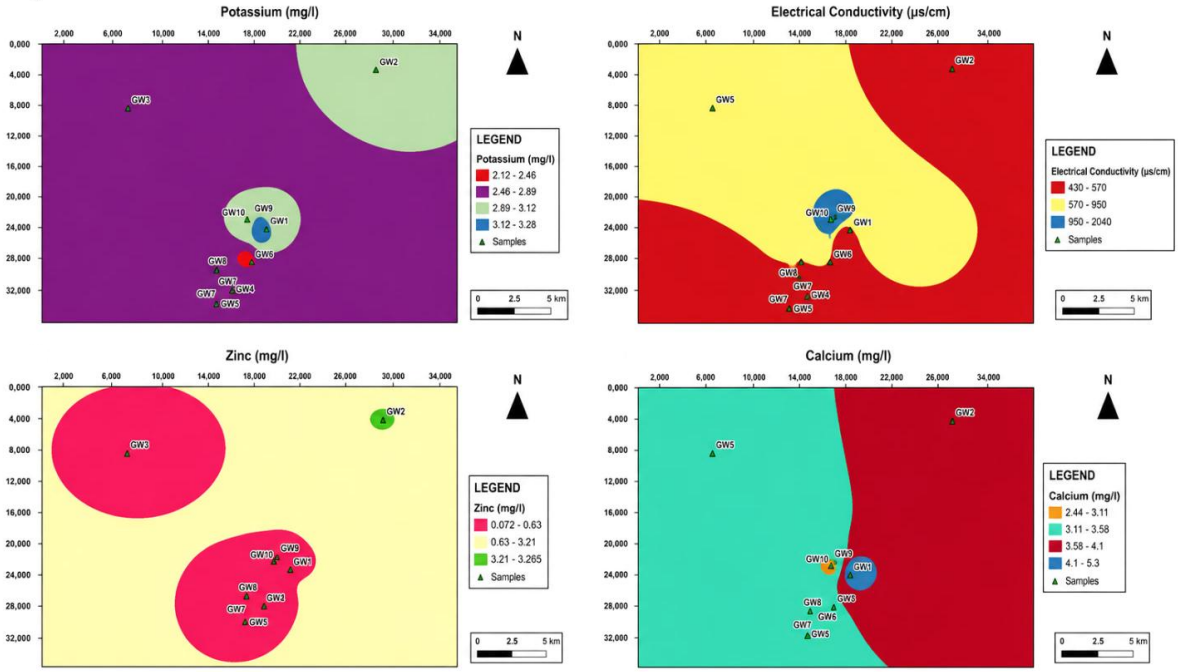

Figure 18. Spatial distribution of potassium, electrical conductivity (EC), zinc, and calcium concentrations across the study area

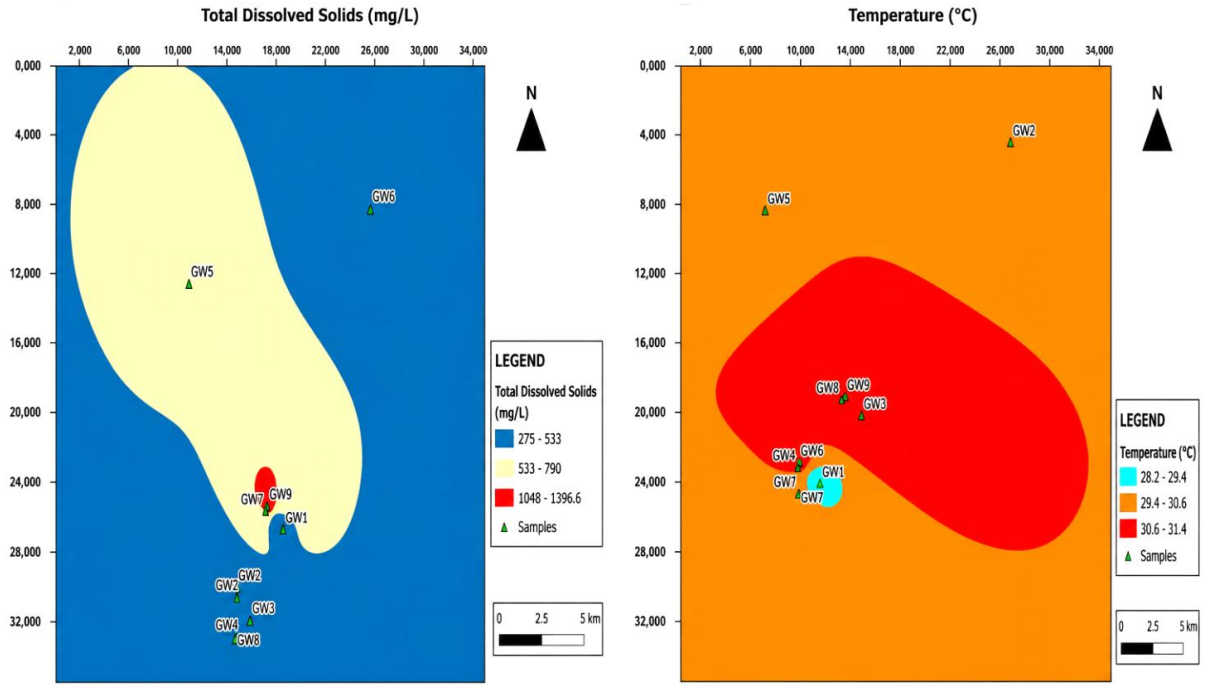

Figure 19. Spatial distribution of total dissolved solids (TDS) and temperature across the study area

Overall, the geospatial maps demonstrate that the hydrochemical parameters are not uniformly distributed across the study area. The observed spatial variability provides a visual representation of differences in groundwater composition among the sampling locations and complements the hydrochemical and statistical results presented in the preceding sections. However, the interpolated patterns alone do not establish specific contamination sources or transport pathways.

DISCUSSION

Hydrogeochemical evolution and petroleum contamination

The predominance of Mg–SO_4 hydrogeochemical facies represents a marked departure from the Ca–HCO_3 facies generally expected in relatively fresh, uncontaminated tropical coastal aquifers, suggesting substantial modification of groundwater chemistry. Elevated zinc, copper, and sodium concentrations, together with increased alkalinity, are consistent with hydrochemical alterations reported in petroleum-impacted groundwater systems (Ogeleka et al., 2017; Alfaifi et al., 2021). The development of Mg–SO_4 facies may reflect mixing between background groundwater and chemically modified waters associated with petroleum production; however, this facies alone does not uniquely identify petroleum-derived formation water, because sulphate and magnesium may also be supplied by mineral dissolution, anthropogenic inputs, or other salinity sources. Similar hydrochemical modifications have been reported in petroleum-impacted aquifers in Saudi Arabia (Alfaifi et al., 2021) and Egypt (Ewida, 2014).

PCA results are broadly consistent with this interpretation, although PCA alone cannot establish contamination sources. PC1 (46.65% variance), characterised by high loadings for Zn, Cu, and Mg, defines a hydrochemical association that is compatible with the influence of petroleum production activities. Zinc may be associated with drilling and production materials, including water-based drilling muds and mineral oils, whereas copper may be derived from metallic infrastructure, waste lubricants, and other production-related inputs (Onwuka et al., 2018). Nevertheless, these elements are not source-specific and may also reflect other anthropogenic or geogenic inputs. PC2 represents a geochemical salinity gradient and may indicate groundwater mineralisation associated with mixing with saline or formation waters, although alternative salinity sources cannot be excluded. PC3, characterised by sulphate–phosphate enrichment, may reflect sulphate inputs associated with petroleum-related processes in combination with other potential anthropogenic nutrient sources. Taken together, the three components provide converging hydrochemical evidence for anthropogenic modification of groundwater that is consistent with petroleum-related influence. Importantly, however, the PCA results should be interpreted as supporting rather than definitive evidence of petroleum contamination, and source attribution should ideally be corroborated by additional hydrochemical, isotopic, or petroleum-specific indicators.

Heavy metal contamination dynamics and ecological risks

Elevated iron concentrations (2.84–12.45 mg/L), corresponding to approximately 9–41 times the WHO guideline value, are likely controlled by multiple interacting processes, including corrosion of steel petroleum infrastructure releasing dissolved ferrous iron, inputs from drilling muds and completion fluids, and mobilisation of naturally occurring sedimentary iron under reducing conditions associated with hydrocarbon degradation (Alloway, 2013; Sracek et al., 2004). In petroleum-impacted aquifers, oxygen depletion resulting from hydrocarbon oxidation can promote the reduction of Fe^{3+} to the more mobile Fe^{2+} species, thereby enhancing iron mobility in groundwater systems (Fetter, 1999).

The observed positive correlation between Zn and Cu ($r = 0.712$) suggests their potential co-occurrence, which may be associated with petroleum production activities and corrosion-related inputs from infrastructure materials (Onwuka et al., 2018). However, correlation analysis alone does not establish a definitive source linkage and should therefore be interpreted in conjunction with spatial and hydrochemical evidence.

Spatial trends showing increasing metal concentrations toward petroleum infrastructure (Cluster 2 > Cluster 1 > Cluster 3; based on hierarchical cluster analysis results) suggest a possible anthropogenic influence, although natural geochemical heterogeneity may also contribute to the observed distribution

patterns. These findings are broadly consistent with previous studies in the Niger Delta region reporting distance-dependent contamination gradients in groundwater systems (Wekpe et al., 2024; Ola et al., 2024).

From an ecological engineering perspective, elevated concentrations of Fe, Mn, Zn, and Cu may pose risks to coastal aquifer–surface water interfaces and associated ecosystems. Iron and manganese precipitation in discharge zones may lead to visible staining and increased oxygen demand, potentially affecting benthic habitat quality. Zinc and copper are recognized as potentially toxic trace metals to aquatic organisms at elevated concentrations, with effects dependent on speciation, bioavailability, and exposure duration (Onwuka et al., 2018). Bioaccumulation in aquatic food webs may represent a potential pathway for transfer to higher trophic levels, including human consumers of fishery resources.

Overall, the results suggest a combined influence of geogenic and anthropogenic processes on groundwater chemistry, with petroleum infrastructure likely contributing to localized enrichment patterns.

Total suspended solids and overall water quality degradation

TSS emerged as the dominant WQI driver (35–55% of index values), with concentrations of 145–520 mg/L exceeding the WHO guideline value by 6–21-fold. Multiple petroleum-related mechanisms may contribute to these elevated concentrations, including drilling operations that suspend fine sediments and drilling waste particles; pipeline construction and maintenance that disturb subsurface sediments; oil-induced changes in interfacial properties that may mobilise otherwise stable sediment aggregates; and erosion associated with petroleum infrastructure placement and operational activities (Alao et al., 2025). High TSS may impair aquifer permeability over time through progressive clogging of pore spaces, potentially creating long-term hydrogeological consequences that extend beyond the operational period of contamination.

Electrical conductivity exceedances (580–1,840 µS/cm; WHO limit: 500 µS/cm) and elevated TDS (1,082–2,338 mg/L) reflect dissolved ion enrichment that may be associated with petroleum formation brines. These brines, with TDS often exceeding 100,000 mg/L in source formations, can substantially increase aquifer conductivity even when considerably diluted (Alsuhaimi et al., 2019). The pH range (6.6–8.4) remained within acceptable WHO bounds (6.5–8.5) across all samples, potentially reflecting the carbonate buffering capacity of the coastal aquifer, which may attenuate pH perturbations associated with petroleum hydrocarbon degradation.

Comparative analysis with published literature

These findings are consistent with, and extend, the body of contamination evidence reported across the Niger Delta. The UNEP (2011) assessment of Ogoniland documented benzene concentrations exceeding WHO guideline values by more than 900-fold and widespread groundwater contamination across an area of approximately 1,000 km²; the present study extends this body of evidence by providing a focused characterisation of the offshore depobelt, a hydrogeological setting that has received comparatively limited attention in previous investigations. Ola et al. (2024) reported TPH concentrations ranging from 3–473 mg/L in Niger Delta groundwater based on sub-catchment assessments; the concentrations observed in the present offshore study indicate comparable contamination severity in an offshore setting. Wekpe et al. (2024) applied source–pathway–receptor modelling to assess contamination risks from crude oil spillages and identified spatial patterns of distance-dependent attenuation, broadly paralleling the cluster structures observed in this study.

The Mg–SO_4 facies documented here has also been reported in petroleum-impacted coastal aquifers in Saudi Arabia (Alfaifi et al., 2021), Egypt (Ewida, 2014), and south-eastern Nigeria (Egbueri & Unigwe, 2020). These similarities support the interpretation of petroleum-related modification of groundwater chemistry, although the Mg–SO_4 facies should not be regarded as uniquely diagnostic of petroleum brine influence. The integrated multi-method framework applied in this study extends previous single-method investigations in the Niger Delta (Omo-Irabor et al., 2018) by providing convergent evidence from five analytical approaches, thereby strengthening the overall interpretation of contamination patterns and their potential sources.

Environmental and engineering implications

Ecological system impacts

The documented groundwater contamination has potentially cascading ecological consequences across the Niger Delta deltaic ecosystem. Contaminated groundwater discharging to surface water bodies may introduce heavy metals and total petroleum hydrocarbons into estuarine and mangrove environments, with potential effects including physiological stress, bioaccumulation, and biodiversity loss. Previous studies have documented substantial declines in fish populations and extensive mangrove degradation in petroleum-impacted Niger Delta waters (Ite et al., 2013). The Mg–SO_4-dominated chemistry observed across all wells indicates a systemic alteration of shallow aquifer geochemistry, with potential implications for wetland plant communities dependent on groundwater baseflow chemistry and for invertebrate communities inhabiting riparian sediments.

The economic costs of environmental degradation in the Niger Delta have been estimated at USD 758 million annually, with 75% borne by local communities through losses of clean water, agricultural productivity, and fisheries-based livelihoods (Sam et al., 2020). More than 1,500 communities across eight crude oil-producing states are reported to be affected, underscoring the scale of the public health and ecological challenges and the need for immediate and sustained engineering intervention (Yakubu, 2023).

Engineering-based remediation recommendations

The spatial contamination maps (Figures 10–19) and cluster analysis results provide actionable engineering information for targeted remediation. Based on the observed spatial distribution and hydrochemical characteristics, four engineering intervention priorities are proposed:

Priority Tier 1 – Immediate Containment (Cluster 2 Wells; 0–500 m from infrastructure): Installation of permeable reactive barriers (PRBs) incorporating zero-valent iron (ZVI)-based reactive media may provide an appropriate in-situ option for immobilisation and removal of dissolved metals, including Fe, Zn, Cu, and Cr, subject to site-specific hydrogeological and geochemical assessment (Song et al., 2021; Obiri-Nyarko, 2014). ZVI-based PRBs have been widely investigated for groundwater remediation, although their hydraulic performance and long-term reactivity require consideration during design because corrosion products and mineral precipitation may reduce permeability (Obiri-Nyarko, 2014). Organoclay-based sorptive media may additionally be considered for petroleum hydrocarbon capture, given their demonstrated affinity for petroleum hydrocarbons and their potential application in groundwater remediation (Ugochukwu et al., 2014).

Pump-and-treat systems, potentially incorporating ion-exchange or other selective treatment processes, may be considered at GW2, GW10, and GW7, identified as the three most contaminated wells, for control of elevated dissolved-ion concentrations. Treatment selection should be based on the specific ionic composition and hydrochemical characteristics of the extracted groundwater. Performance should be monitored at approximately 3-month intervals using the parameter suite analysed in this study, with monitoring frequency adjusted according to treatment performance and regulatory requirements.

Priority Tier 2 – Source Control and Infrastructure Engineering (All Clusters): Mandatory replacement of petroleum pipelines older than 20 years, or replacement in accordance with applicable integrity-management standards and site-specific assessment, depending on pipe material, corrosion protection, operating conditions, and maintenance history. Pipeline age is an important factor in deterioration and failure assessment, but corrosion rate, operating conditions, defect characteristics, and maintenance history should also be incorporated into decisions regarding repair or replacement (Cui & Wang, 2014; Huang et al., 2023). Continuous fibre-optic leak-detection systems should be considered along priority pipeline corridors, particularly where groundwater contamination is spatially associated with petroleum infrastructure. Secondary containment for storage facilities and closed-loop drilling systems should likewise be prioritised to reduce the potential for releases of petroleum and drilling-related wastes to the surrounding environment.

Priority Tier 3 – Bioremediation and Natural Attenuation Enhancement (Cluster 1 and Cluster 3 Wells): Enhanced in-situ bioremediation using nutrient amendment (N and P) may be considered where hydrochemical and microbiological conditions are favourable for stimulation of indigenous hydrocarbon-degrading communities. Field-scale research has demonstrated that nitrate and phosphate amendment can stimulate petroleum hydrocarbon degradation in contaminated aquifers, although treatment effectiveness is strongly dependent on aquifer conditions and contaminant distribution (Ponsin et al., 2014). Where contaminant concentrations show a sustained downward trend, monitored natural attenuation should be considered as a complementary management strategy. Quarterly monitoring may be used to assess contaminant trends and verify the progression of attenuation processes.

Priority Tier 4 – Alternative Water Supply (All Communities): Development of deeper and hydraulically isolated groundwater resources may be considered as an alternative water-supply strategy, subject to detailed hydrogeological assessment of aquifer connectivity, yield, and vulnerability to contamination. Community-scale treatment trains should be selected according to the measured contaminant profile and may include coagulation–flocculation for suspended solids, activated carbon or other sorptive media for petroleum-derived organic compounds, and membrane-based treatment such as reverse osmosis where dissolved solids and metal concentrations require substantial reduction. Household point-of-use treatment may provide an interim risk-reduction measure while long-term groundwater restoration and source-control measures are implemented.

Monitoring and environmental management framework

An evidence-based environmental monitoring programme is recommended with the following architecture:

(i) Monthly groundwater sampling at Cluster 2 wells and quarterly sampling at Cluster 1 and Cluster 3 wells, analysing the full parameter suite used in this study, supplemented by BTEX and PAH compounds;

(ii) Real-time continuous logging of pH, EC, temperature, and dissolved oxygen at Cluster 2 wells using multi-parameter data sondes with cloud-based telemetry and automated alert systems, where technically and financially feasible;

(iii) Annual GIS-based updates of spatial contamination maps using the IDW framework established in this study, enabling detection of temporal trends in contaminant distribution;

(iv) Establishment of community-based monitoring committees with appropriate technical training and equipment, providing local oversight and contributing to early warning of new spill events.

Regulatory and policy engineering relevance

The WQI findings, with all ten wells classified as Unsuitable, provide a clear basis for prioritising regulatory attention and environmental management intervention. The findings are relevant to the environmental requirements established under the Environmental Guidelines and Standards for the Petroleum Industry in Nigeria (EGASPIN; DPR, 2002), as well as the post-Petroleum Industry Act (PIA) regulatory framework administered by the Nigerian Upstream Petroleum Regulatory Commission (NUPRC). In particular, the Upstream Petroleum Environmental Regulations 2022 establish requirements for environmental monitoring, effluent control, pollution prevention, and remediation-related activities, while the Nigerian Upstream Petroleum Environmental Remediation Regulations 2024 provide a more specific framework for environmental remediation in the upstream petroleum sector (Federal Republic of Nigeria, 2024).

The magnitude and spatial distribution of the exceedances documented in this study therefore provide scientifically relevant evidence for regulatory assessment, prioritisation of affected areas, and investigation of potential pollution sources and responsible operators. The integrated spatial maps generated in this study may further support regulatory inspections, environmental risk assessment, remediation planning, and, where appropriate, subsequent enforcement or legal processes. However, attribution of responsibility and determination of regulatory or legal liability require independent verification in accordance with applicable regulatory procedures.

Internationally, the findings support alignment with the United Nations Sustainable Development Goal 6 (Clean Water and Sanitation) and SDG 15 (Life on Land), particularly their objectives concerning the reduction of water pollution, protection of freshwater resources, and conservation of terrestrial and aquatic ecosystems. The methodology developed here offers a potentially replicable framework for environmental compliance monitoring and groundwater-quality assessment by regulatory agencies and petroleum operators in Nigeria and, with appropriate site-specific adaptation, in analogous petroleum-producing basins in West Africa, Southeast Asia, and South America.

Overall, the integration of WQI assessment, spatial mapping, hydrogeochemical characterisation, cluster analysis, and contaminant evaluation provides a practical evidence base for linking groundwater-quality assessment with regulatory decision-making and environmental management in petroleum-impacted environments.

Management implications and future research directions

The findings of this study have several implications for groundwater quality management in petroleum-impacted environments. The observed spatial variability in hydrochemical parameters and the clustering of elevated

contaminant levels near infrastructure suggest that monitoring strategies should prioritise areas in close proximity to operational facilities. In particular, enhanced and more frequent groundwater quality surveillance in such zones, including the inclusion of organic contaminants such as BTEX and PAHs, would improve early detection of emerging pollution signals and support more adaptive management frameworks.

Where elevated contamination levels were identified, particularly within the most impacted clusters, the results indicate a potential need for site-specific remediation planning. In similar hydrogeological settings, technologies such as permeable reactive barriers and pump-and-treat systems have been widely applied, although their effectiveness depends strongly on local hydrogeochemical conditions and long-term maintenance requirements. Continuous performance monitoring is therefore essential to evaluate remediation efficiency over time.

The results further highlight the importance of infrastructure integrity in preventing subsurface contamination. Ageing pipelines and storage systems have been widely recognised as potential sources of chronic leakage in petroleum-producing regions. Consequently, systematic inspection, integrity assessment, and progressive upgrading of infrastructure, combined with improved leak detection technologies and secondary containment measures, may significantly reduce future contaminant inputs to groundwater systems.

From a governance perspective, effective protection of groundwater resources requires not only technical interventions but also strengthened regulatory oversight and timely response mechanisms. Real-time monitoring of effluent quality and transparent reporting systems could improve compliance and reduce delays in identifying pollution events. In addition, contingency planning for alternative water supply options is important in areas where groundwater resources are already affected, particularly for vulnerable communities dependent on shallow aquifers.

Community participation may also play an important role in long-term environmental management. Locally engaged monitoring initiatives, supported by appropriate technical training and accessible reporting frameworks, can enhance data coverage and contribute to earlier identification of pollution events, while also improving communication and trust among stakeholders.

Finally, this study underscores the need for the development of comprehensive baseline hydrogeochemical datasets and long-term monitoring programmes in the Niger Delta region. Such datasets, combined with predictive modelling approaches, would support improved understanding of contaminant transport processes, facilitate risk-based decision-making, and contribute to more sustainable groundwater resource management in petroleum-impacted environments.

CONCLUSION

This study achieved its objective of providing an integrated hydrogeochemical assessment of groundwater quality in the offshore Niger Delta depobelt by combining hydrogeochemical facies analysis, multivariate statistical techniques, water quality indices, and geospatial analysis within a single analytical framework. The findings support the working hypothesis that groundwater quality in the investigated offshore field is substantially influenced by hydrochemical processes associated with petroleum production activities, although natural hydrogeochemical processes also contribute to the observed variability.

The results demonstrated that groundwater throughout the study area is characterised predominantly by a magnesium–sulphate hydrogeochemical facies, indicating a substantial deviation from the calcium–bicarbonate water type typically associated with relatively unimpacted coastal aquifers. Multivariate statistical analysis further revealed three principal hydrochemical patterns related to groundwater mineralisation, salinity, and sulphate–phosphate enrichment, while hierarchical cluster analysis identified distinct groups of sampling locations exhibiting different levels of groundwater quality deterioration.

Water quality assessment indicated that all investigated groundwater samples exceeded the acceptable threshold for drinking purposes according to the calculated Water Quality Index, whereas the Metal Index identified varying degrees of metal contamination, with iron and total suspended solids representing the principal contributors to groundwater quality degradation. Geospatial analysis additionally identified areas located in close proximity to petroleum infrastructure as priority zones for groundwater monitoring and remediation.

The principal scientific contribution of this study lies in demonstrating the applicability of an integrated hydrogeochemical assessment framework for evaluating groundwater quality in offshore petroleum-producing environments, where previous investigations have been comparatively limited. By combining complementary graphical, statistical, index-based, and spatial analytical approaches, the study provides a more comprehensive understanding of groundwater hydrochemistry than can be achieved using any individual method alone. Consequently, the research contributes to addressing the existing knowledge gap regarding offshore groundwater quality in the Niger Delta and offers a methodological framework that can be adapted for groundwater assessment in comparable petroleum-producing sedimentary basins.

Although the results consistently suggest an association between groundwater quality deterioration and petroleum production activities, the relatively limited number of sampling locations and the single-season sampling campaign constrain definitive source attribution and assessment of long-term groundwater evolution. Future studies should therefore incorporate larger monitoring networks, multi-season observations, and direct petroleum-specific tracers to further strengthen source attribution and improve understanding of groundwater quality dynamics over time.

Author's statements

Contributions

Conceptualisation: I.E.O.; Data curation: N.A.C.; Formal analysis: N.A.C., M.A.A.; Investigation: N.A.C., C.S.A.; Methodology: I.E.O., M.A.O.; Project administration: I.E.O.; Resources: I.C.C.; Software: N.A.C.; Supervision: I.E.O.; Validation: E.I.O.; Visualization: J.E.; Writing – original draft: N.A.C.; Writing – review & editing: N.A.C., M.A.O.

Declaration of conflicting interest

The authors declare no competing interests.

Financial interests

The authors declare they have no financial interests.

Funding

Not applicable.

Data availability statement

Data used for the study would be made available on request.

AI Disclosure

Generative AI tools were used solely for language editing and proofreading. The authors take full responsibility for the manuscript's content, analysis, interpretations, and conclusions.

Ethical approval declarations

Not applicable.

Additional information

Publisher's note

Publisher remains neutral with regard to jurisdictional claims in published maps and institutional affiliations.

REFERENCES

Akakuru, O. C., Akudinobi, B., Opara, A. I., Onyekuru, S. O., & Akakuru, O. U. (2021). Hydrogeochemical facies and pollution status of groundwater resources of Owerri and environs, Southeastern Nigeria. *Environmental Monitoring and Assessment*, 193(10), 623. https://doi.org/10.1007/s10661-021-09364-9.

Alao, J. O., Abdulsalami, M., Mohammed, M. A., & Eze, S. U. (2025). Groundwater contamination due to hydrocarbon extraction activities in the Niger Delta: A potential challenge towards sustainable environment and public health. *Water-Energy Nexus*, 9, 93–108. https://doi.org/10.1016/j.wen.2025.12.002.

Alfaifi, H., El-Sorogy, A. S., Qaysi, S., Kahal, A., Almadani, S., Alshehri, F., & Zaidi, F. K. (2021). Evaluation of heavy metal contamination and groundwater quality along the Red Sea coast, southern Saudi Arabia. *Marine Pollution Bulletin*, 163, 111975. http://dx.doi.org/10.1016/j.marpolbul.2021.111975.

Alloway, B.J. (2013) *Heavy Metals in Soils: Trace Metals and Metalloids in Soils and their Bioavailability*. 3rd edn. Dordrecht: Springer.

AlSuhaimi, A. O., AlMohaimidi, K. M., & Momani, K. A. (2019). Preliminary assessment for physicochemical quality parameters of groundwater in Oqdus Area, Saudi Arabia. *Journal of the Saudi Society of Agricultural Sciences*, 18(1), 22–31. https://doi.org/10.1016/j.jssas.2016.12.002.

American Public Health Association. (2017). *Standard methods for the examination of water and wastewater (23rd ed.)*. American Public Health Association.

Barcelona, M. J. (1985). *Practical guide for ground-water sampling* (Vol. 600, No. 2–104). Robert S. Kerr Environmental Research Laboratory, Office of Research and Development, US Environmental Protection Agency.

Cui, B., & Wang, H. (2024). Pipeline corrosion prediction and uncertainty analysis with an ensemble Bayesian neural network approach. *Process Safety and Environmental Protection*, 187, 483–494. https://doi.org/10.1016/j.psep.2024.05.011.

Durov, S. A. (1948). *Natural waters and graphic representation of their composition*. In Dokl Akad Nauk SSSR (Vol. 59, No. 3, pp. 87–90).

Edet, A. E., & Offiong, O. E. (2002). Evaluation of water quality pollution indices for heavy metal contamination monitoring. A study case from Akpabuyo-Odukpani area, Lower Cross River Basin (southeastern Nigeria). *GeoJournal*, 57(4), 295–304. https://doi.org/10.1023/B:GEJO.0000007250.92458.de.

Egbueri, J. C., & Unigwe, C. O. (2020). Understanding the extent of heavy metal pollution in drinking water supplies from Umunya, Nigeria: an indexical and statistical assessment. Analytical Letters, 53(13), 2122–2144. https://doi.org/10.1080/00032719.2020.1731521.

El-Rawy, M., Wahba, M., Fathi, H., Alshehri, F., Abdalla, F., & El Attar, R. M. (2024). Assessment of groundwater quality in arid regions utilizing principal component analysis, GIS, and machine learning techniques. *Marine Pollution Bulletin*, 205, 116645. https://doi.org/10.1016/j.marpolbul.2024.116645.

Evamy, B. D., Haremboure, J., Kamerling, P., Knaap, W. A., Molloy, F. A., & Rowlands, P. H. (1984). *Hydrocarbon habitat of Tertiary Niger delta*. In Petroleum Geochemistry and Basin Evaluation. Editor(s) Gerard Demaison; Roelef J. Murris. https://doi.org/10.1306/M35439C19.

Ewida, A. Y. (2014). Oil spills: Impact on water quality and microbial community on the Nile River, Egypt. *International Journal of Environmental Research and Public Health*, 3(4), 192–198. https://www.curresweb.com/ije/ije/2014/192-198.pdf.

Ewim, D. R. E., Orikpete, O. F., Scott, T. O., Onyebuchi, C. N., Onukogu, A. O., Uzougbo, C. G., & Onunka, C. (2023). Survey of wastewater issues due to oil spills and pollution in the Niger Delta area of Nigeria: a secondary data analysis. *Bulletin of the National Research Centre*, 47(1), 116. https://doi.org/10.1186/s42269-023-01090-1.

Federal Republic of Nigeria. (2024). *Nigerian upstream petroleum environmental remediation regulations*, 2024. Nigerian Upstream Petroleum Regulatory Commission. https://www.nuprc.gov.ng/upload/nuprc_laws/Nigerian_Upstream_Petroleum_Environmental_Remediation_Regulations_2024_981b03c9dc2fad23436bdfe2.pdf.

Fetter, C. W. (1999). *Contaminant hydrogeology, 2nd edn*. Prentice Hall, Upper Saddle River, NJ.

Food and Agriculture Organization of the United Nations. (2020). *AQUASTAT database*. https://www.fao.org/aquastat/.

Gad, M., Gaagai, A., Eid, M. H., Szűcs, P., Hussein, H., Elsherbiny, O., ... & Ibrahim, H. (2023). Groundwater quality and health risk assessment using indexing approaches, multivariate statistical analysis, artificial neural networks, and GIS techniques in El Kharga Oasis, Egypt. *Water*, 15(6), 1216. https://doi.org/10.3390/w15061216.

Gautam, V. K., Kothari, M., Al-Ramadan, B., Singh, P. K., Upadhyay, H., Pande, C. B., ... & Yaseen, Z. M. (2024). Groundwater quality characterization using an integrated water quality index and multivariate statistical techniques. *PLoS one*, 19(2), e0294533. https://doi.org/10.1371/journal.pone.0294533.

Harper, D. A. (2001). PAST: paleontological statistics software package for education and data analysis. *Palaeontol. Electron.*, 4, 4. http://palaeo-electronica.org/2001_1/past/issue1_01.htm.

Horton, R. K. (1965). An index number system for rating water quality. *Journal of Water Pollution Control Federation*, 37(3), 300–306.

Huang, Y., Qin, G., & Yang, M. (2023). A risk-based approach to inspection planning for pipelines considering the coupling effect of corrosion and dents. *Process Safety and Environmental Protection*, 180, 588–600. https://doi.org/10.1016/j.psep.2023.10.025.

Ite, A. E., Ibok, U. J., Ite, M. U., & Petters, S. W. (2013). Petroleum exploration and production: Past and present environmental issues in the Nigeria's Niger Delta. *American Journal of Environmental Protection*, 1(4), 78–90. https://doi.org/10.12691/env-1-4-2.

Liu, C. W., Lin, K. H., & Kuo, Y. M. (2003). Application of factor analysis in the assessment of groundwater quality in a blackfoot disease area in Taiwan. *Science of the Total Environment*, 313(1–3), 77–89. https://doi.org/10.1016/S0048-9697(02)00683-6.

Obiri-Nyarko, F., Grajales-Mesa, S. J., & Malina, G. (2014). An overview of permeable reactive barriers for in situ sustainable groundwater remediation. *Chemosphere*, 111, 243–259. https://doi.org/10.1016/j.chemosphere.2014.03.112.

Ogeleka, D. F., Tudararo-Aherobo, L. E., & Okieimen, F. E. (2017). Ecological effects of oil spill on water and sediment from two riverine communities in Warri, Nigeria. *International Journal of Biological and Chemical Sciences*, 11(1), 453–461. http://dx.doi.org/10.4314/ijbcs.v11i1.36.

Ola, I., Drebenstedt, C., Burgess, R. M., Mensah, M., Hoth, N., Okoroafor, P., & Külls, C. (2024). Assessing petroleum contamination in parts of the Niger Delta based on a sub-catchment delineated field assessment. *Environmental Monitoring and Assessment*, 196(6), 585. https://doi.org/10.1007/s10661-024-12743-7.

Omo-irabor, O. M. O., Izeze, E. O., & Akpere, O. (2018). Assessment of heavy metal contamination in groundwater of Agbor, Ika south l. GA, delta state, Nigeria. *Pacific International Journal*, 1(4), 184–191. https://doi.org/10.55014/pij.v1i4.55.

Onwuka, O. S., Igwe, O., Ifediegwu, S. I., & Uwom, C. S. (2018). An assessment of the effectiveness of drilling waste treatment process in X-gas field, Niger Delta, Nigeria. *Geology, Ecology, and Landscapes*, 2(4), 288–302. https://doi.org/10.1080/24749508.2018.1473751.

Onyena, A. P., & Sam, K. (2020). A review of the threat of oil exploitation to mangrove ecosystem: Insights from Niger Delta, Nigeria. *Global Ecology and Conservation*, 22, e00961. https://doi.org/10.1016/j.gecco.2020.e00961.

Ordinioha, B., & Brisibe, S. (2013). The human health implications of crude oil spills in the Niger delta, Nigeria: An interpretation of published studies. *Nigerian Medical Journal: Journal of the Nigeria Medical Association*, 54(1), 10. https://doi.org/10.4103/0300-1652.108887.

Oyebamiji, A. R., Hoque, M. A., & Whitworth, M. (2025). Regional assessment of groundwater contamination risk from crude oil spillages in the Niger Delta: a novel application of the source-pathway-receptor model. *Earth Systems and Environment*, 9(1), 117–133. https://doi.org/10.1007/s41748-024-00416-x.

Piper, A. M. (1944). A graphic procedure in the geochemical interpretation of water-analyses. *Eos, Transactions American Geophysical Union*, 25(6), 914–928. https://doi.org/10.1029/TR025i006p00914.

Ponsin, V., Coulomb, B., Guelorget, Y., Maier, J., & Höhener, P. (2014). In situ biostimulation of petroleum hydrocarbon degradation by nitrate and phosphate injection using a dipole well configuration. *Journal of Contaminant Hydrology*, 171, 22–31. https://doi.org/10.1016/j.jconhyd.2014.10.003.

Sam, K., Coulon, F., & Prpich, G. (2017). Management of petroleum hydrocarbon contaminated sites in Nigeria: Current challenges and future direction. *Land Use Policy*, 64, 133–144. https://doi.org/10.1016/j.landusepol.2017.01.051.

Shepard, D. (1968, January). *A two-dimensional interpolation function for irregularly-spaced data*. In Proceedings of the 1968 23rd ACM national conference (pp. 517–524). https://doi.org/10.1145/800186.810616.

Short, K. C., & Stäuble, A. J. (1967). Outline of geology of Niger Delta. *AAPG bulletin*, 51(5), 761–779. https://doi.org/10.1306/5D25C0CF-16C1-11D7-8645000102C1865D.

Song, J., Huang, G., Han, D., Hou, Q., Gan, L., & Zhang, M. (2021). A review of reactive media within permeable reactive barriers for the removal of heavy metal (loid) s in groundwater: Current status and future prospects. *Journal of Cleaner Production*, 319, 128644. https://doi.org/10.1016/j.jclepro.2021.128644.

Sracek, O., Bhattacharya, P., Jacks, G., Gustafsson, J. P., & Von Brömssen, M. (2004). Behavior of arsenic and geochemical modeling of arsenic enrichment in aqueous environments. *Applied Geochemistry*, 19(2), 169–180. https://doi.org/10.1016/j.apgeochem.2003.09.005.

Stiff Jr, H. A. (1951). The interpretation of chemical water analysis by means of patterns. *Journal of Petroleum Technology*, 3(10), 15–17. https://doi.org/10.2118/951376-G.

Taşan, M., Demir, Y., & Taşan, S. (2022). Groundwater quality assessment using principal component analysis and hierarchical cluster analysis in Alaçam, Turkey. *Water Supply*, 22(3), 3431–3447. https://doi.org/10.2166/ws.2021.390.

Ugochukwu, U. C., Manning, D. A., & Fialips, C. I. (2014). Microbial degradation of crude oil hydrocarbons on organoclay minerals. *Journal of Environmental Management*, 144, 197–202. https://doi.org/10.1016/j.jenvman.2014.06.002.

United Nations Development Programme. (2006). *Niger Delta human development report*. United Nations Development Programme.

United Nations Environment Programme. (2011). *Environmental assessment of Ogoniland*. United Nations Environment Programme.

Weber, K. J. (1975). *Petroleum geology of the Niger Delta*. Proceed. 9th World Petrol. Congr., 2, 209–221.

World Health Organization. (2011). *Guidelines for drinking-water quality* (4th ed.). World Health Organization. https://www.who.int/publications/i/item/9789241549950.